



University of Kentucky
UKnowledge

Theses and Dissertations--Biosystems and
Agricultural Engineering

Biosystems and Agricultural Engineering


2021

Extraction of Micro- and Nano-Plastic Particles from Water Using Hydrophobic Natural Deep Eutectic Solvents

Jameson R. Hunter

University of Kentucky, jameson.hunter9@gmail.com

Author ORCID Identifier:

 <https://orcid.org/0000-0002-4102-7803>

Digital Object Identifier: <https://doi.org/10.13023/etd.2021.385>

[Right click to open a feedback form in a new tab to let us know how this document benefits you.](#)

Recommended Citation

Hunter, Jameson R., "Extraction of Micro- and Nano-Plastic Particles from Water Using Hydrophobic Natural Deep Eutectic Solvents" (2021). *Theses and Dissertations--Biosystems and Agricultural Engineering*. 83.

https://uknowledge.uky.edu/bae_etds/83

This Master's Thesis is brought to you for free and open access by the Biosystems and Agricultural Engineering at UKnowledge. It has been accepted for inclusion in Theses and Dissertations--Biosystems and Agricultural Engineering by an authorized administrator of UKnowledge. For more information, please contact UKnowledge@lsv.uky.edu.

STUDENT AGREEMENT:

I represent that my thesis or dissertation and abstract are my original work. Proper attribution has been given to all outside sources. I understand that I am solely responsible for obtaining any needed copyright permissions. I have obtained needed written permission statement(s) from the owner(s) of each third-party copyrighted matter to be included in my work, allowing electronic distribution (if such use is not permitted by the fair use doctrine) which will be submitted to UKnowledge as Additional File.

I hereby grant to The University of Kentucky and its agents the irrevocable, non-exclusive, and royalty-free license to archive and make accessible my work in whole or in part in all forms of media, now or hereafter known. I agree that the document mentioned above may be made available immediately for worldwide access unless an embargo applies.

I retain all other ownership rights to the copyright of my work. I also retain the right to use in future works (such as articles or books) all or part of my work. I understand that I am free to register the copyright to my work.

REVIEW, APPROVAL AND ACCEPTANCE

The document mentioned above has been reviewed and accepted by the student's advisor, on behalf of the advisory committee, and by the Director of Graduate Studies (DGS), on behalf of the program; we verify that this is the final, approved version of the student's thesis including all changes required by the advisory committee. The undersigned agree to abide by the statements above.

Jameson R. Hunter, Student

Dr. Jian Shi, Major Professor

Dr. Donald Colliver, Director of Graduate Studies

EXTRACTION OF MICRO- AND NANO-PLASTIC PARTICLES FROM WATER
USING HYDROPHOBIC NATURAL DEEP EUTECTIC SOLVENTS

THESIS

A thesis submitted in partial fulfillment of the
requirements for the degree of Master of Science in
Biosystems and Agricultural Engineering in the
Colleges of Agriculture and Engineering
at the University of Kentucky

By

Jameson Hunter

Lexington, Kentucky

Director: Dr. Jian Shi, Associate Professor of Biosystems and Agricultural Engineering

Lexington, Kentucky

2021

Copyright © Jameson Hunter 2021
<https://orcid.org/0000-0002-4102-7803>

ABSTRACT OF THESIS

EXTRACTION OF MICRO- AND NANO-PLASTIC PARTICLES FROM WATER USING HYDROPHOBIC NATURAL DEEP EUTECTIC SOLVENTS

The production of plastic and the amount of waste plastic that enters the environment increases every year. Synthetic polymers will gradually break down into particles on the micro- and nano-scale. The micro- and nano-plastics pose a significant ecological harm by transporting toxic chemicals and causing inflammation and cellular damage when ingested. Two common plastics are polyethylene terephthalate (PET) and Polystyrene (PS), and a newer bioplastic polylactic acid (PLA) that has become a popular alternative. Deep eutectic solvents are a recently discovered solvent composed of a hydrogen bond donor and hydrogen bond acceptor and have been proposed as a cheaper alternative to ionic liquids. Hydrophobic varieties of natural DES (NADES) have been used as extractants in liquid-liquid extractions. The aim of this study is to investigate the relationship between three NADES and micro- and nano-plastics in a liquid-liquid extraction system. The results show that all three NADES extracted plastic particles in the range of 55%-83% with varying rates of extraction. The conclusions from this study are that the plastic particles have a higher affinity for NADES than water and may extract at different rates, but the maximum percentage of plastic particles extracted does not vary significantly.

KEYWORDS: Deep Eutectic Solvents, Nano-plastic, Polyethylene Terephthalate, Polystyrene, Polylactic Acid, Liquid-liquid extraction

Jameson Hunter

(Name of Student)

09/20/2021

Date

EXTRACTION OF MICRO- AND NANO-PLASTIC PARTICLES FROM WATER
USING HYDROPHOBIC NATURAL DEEP EUTECTIC SOLVENTS

By
Jameson Hunter

Dr. Jian Shi

Director of Thesis

Dr. Donald Colliver

Director of Graduate Studies

09/20/2021

Date

DEDICATION

To my family, who supported me throughout the entire process, and my friends and colleagues, who helped out in any way they could.

ACKNOWLEDGMENTS

The following thesis, while an individual work, benefited from the insights and direction of several people. First, my Thesis Chair, Jian Shi, exemplifies the high quality scholarship to which I aspire. In addition, the other members of my lab group, Joseph Stevens, Ryan Kalinoski, Wenqi Li, Yuxuan Zhang, Can Liu, and Makua Vin Nnajofofor, who provided timely and instructive comments and evaluation at every stage of the thesis process. Next, I wish to thank the complete Thesis Committee, Czarena Crofcheck and David Rodgers. Each individual provided insights that guided and challenged my thinking, substantially improving the finished product. I would also like to thank Qi Qiao and Qing Shao for their work in collaborating with me and for giving insights and comments to improve this study.

In addition to the technical and instrumental assistance above, I received equally important assistance from family and friends. My sister, Catherine, provided on-going support throughout the thesis process. My parents, other siblings, and close friends also shared support and words of encouragement that played a major role in completing this thesis.

TABLE OF CONTENTS

ACKNOWLEDGMENTS	iii
TABLE OF CONTENTS.....	iv
LIST OF TABLES	vii
LIST OF FIGURES	viii
CHAPTER 1. INTRODUCTION	1
1.1 Plastics	1
1.1.1 Macro-, Micro-, and Nano-Plastic Particles	1
1.1.2 Environmental and Ecological Impacts	2
1.1.3 Pollution Numbers	4
1.1.4 Collection and Control.....	5
1.1.5 Polyethylene Terephthalate.....	7
1.1.6 Polystyrene.....	8
1.1.7 Polylactic Acid.....	9
1.1.8 Deep Eutectic Solvents	9
1.1.9 Recent Development in DES and Application in Compound Extraction	11
1.2 Motivations and Objectives	14
CHAPTER 2. Materials and Methods.....	16
2.1 Materials	16
2.1.1 Chemicals.....	16
2.1.2 Equipment.....	16
2.2 NADES Synthesis.....	17
2.3 NADES Characterization.....	17
2.3.1 Contact Angle Measurements.....	17
2.4 Plastic Particle Preparation	18
2.4.1 Polyethylene Terephthalate.....	18
2.4.2 Polystyrene.....	19
2.4.3 Polylactic Acid.....	19
2.5 Particle Size Distribution and Zeta-Potential Analysis.....	20
2.6 Plastic Particle Extraction.....	20
2.6.1 Determining Plastic Concentration with Optical Density Measurements	20
2.6.2 Polyethylene Terephthalate Extraction.....	20
2.6.3 Extraction of Plastic Particles	21
2.6.4 Salt-water Extraction	21

2.7	Molecular Interaction Simulations.....	22
2.8	Statistical Analysis and Regression	23
2.8.1	Polymers across NADES	23
2.8.2	NADES across Polymers	23
CHAPTER 3. Results and Discussion		24
3.1	Contact Angle Analysis	24
3.2	Particle Size Analysis	29
3.3	Plastic Extraction	33
3.3.1	Concentration of Plastic Particles from Optical Density	33
3.3.2	PET Extraction.....	34
3.3.3	PS Extraction	35
3.3.4	PLA Extraction	36
3.3.5	Salt-water Extraction	37
3.4	Statistical Analysis.....	37
3.4.1	Polymers across NADES	37
3.4.2	NADES across Polymers	39
3.5	Regression Model	39
3.5.1	PET	41
3.5.1.1	Decanoic Acid:Menthol (1:1).....	41
3.5.1.2	Decanoic Acid:Menthol (1:2).....	41
3.5.1.3	Thymol:Menthol (1:1)	42
3.5.1.4	Comparison of Regressions	43
3.5.2	PS	44
3.5.2.1	Decanoic Acid:Menthol (1:1).....	44
3.5.2.2	Decanoic Acid:Menthol (1:2).....	45
3.5.2.3	Thymol:Menthol (1:1)	46
3.5.2.4	Comparison of Regressions	47
3.5.3	PLA.....	48
3.5.3.1	Decanoic Acid:Menthol (1:1).....	48
3.5.3.2	Decanoic Acid:Menthol (1:2).....	49
3.5.3.3	Thymol:Menthol (1:1)	51
3.5.3.4	Comparison of Regressions	52
3.6	Simulation.....	53
3.7	Discussion.....	56
3.7.1	Contact Angle and Wettability.....	57
3.7.2	Simulation.....	58
3.7.3	Particle Size and Zeta Potential	59
CHAPTER 4. Conclusions and Future Work		61

4.1	Conclusions.....	61
4.2	Future Work.....	63
APPENDICES		65
1.	APPENDIX 1: STATISTICAL ANALYSIS TABLES	65
1.1.	Polymer Extraction Tables.....	65
1.2.	Regression Reports	79
1.3.	Contact Angle Tables.....	82
2.	APPENDIX 2: DETAILED SIMULATION METHODOLOGY	86
2.1.	Molecular Model.....	86
2.2.	Simulation Detail	87
3.	APPENDIX 3: ADDITIONAL SIMULATION FIGURES	90
REFERENCES		93
VITA.....		96

LIST OF TABLES

Table 1 Contact angle measurements in degrees	25
Table 2 DLS measurements in DI water with standard error	29
Table 3 DLS measurements in salt-water with standard error.....	31
Table 4 PET Extraction Percent at 2 h and the endpoint	35
Table 5 PS Extraction Percent at 2 hours and the endpoint.....	35
Table 6 PLA Extraction Percent at 20 min and the endpoint	36
Table 7 PET Regression Coefficient Comparison	44
Table 8 PS Regression Coefficient Comparison.....	48
Table 9 PLA Regression Coefficient Comparison.....	52

LIST OF FIGURES

Figure 1 Flow chart of how plastic enters the environment and ecosystem (Gangadoo, Owen et al. 2020).....	4
Figure 2 Chemical Structure of Polyethylene Terephthalate.....	8
Figure 3 Chemical Structure of Polystyrene.....	8
Figure 4 Chemical Structure of Polylactic Acid.....	9
Figure 5 Chemical Structures of (a) Decanoic Acid, (b) Thymol, and (c) Menthol.....	12
Figure 6 Contact angles of a) water, b) decanoic acid:menthol (1:1), c) decanoic acid:menthol (1:2), and d) thymol:menthol (1:1) at 0 seconds (left) and 30 seconds (right) on PET surface.....	26
Figure 7 Contact angles of a) water, b) decanoic acid:menthol (1:1), c) decanoic acid:menthol (1:2), and d) thymol:menthol (1:1) at 0 seconds (left) and 30 seconds (right) on PS surface.....	27
Figure 8 Contact angles of a) water, b) decanoic acid:menthol (1:1), c) decanoic acid:menthol (1:2), and d) thymol:menthol (1:1) at 0 seconds (left) and 30 seconds (right) on PLA surface.	28
Figure 9 Size distributions of plastic particles (PET, PS, and PLA) in DI water.	30
Figure 10 Size distribution for plastic particles (PET, PS, and PLA) in salt-water.....	32
Figure 11 PET Concentration vs Absorbance Correlation	33
Figure 12 PS Concentration vs Absorbance Correlation	34
Figure 13 PLA Concentration vs Absorbance Correlation.....	34
Figure 14 Percent of PET extracted by decanoic acid:menthol (1:1) regression.....	41
Figure 15 Percent of PET extracted by decanoic acid:menthol (1:2) regression.....	42
Figure 16 Percent of PET extracted by thymol:menthol (1:1) regression	43
Figure 17 Percent of PET extracted regression comparison.....	44
Figure 18 Percent of PS extracted by decanoic acid:menthol (1:1) regression	45
Figure 19 Percent of PS extracted by decanoic acid:menthol (1:2) regression	46
Figure 20 Percent of PS extracted by thymol:menthol (1:1) regression.....	47
Figure 21 Percent of PS extracted regression comparison.....	48
Figure 22 Percent of PLA extracted by decanoic acid:menthol (1:1) regression	49
Figure 23 Percent of PLA extracted by decanoic acid:menthol (1:2) failed regression ...	50
Figure 24 Percent of PLA extracted by decanoic acid:menthol (1:2) regression	51
Figure 25 Percent of PLA extracted by thymol:menthol (1:1) regression.....	52
Figure 26 Percent of PLA extracted regression comparison	53

Figure 27 Final configuration and RDF results from the polymers in decanoic acid:menthol (1:1). (a)-(c) show the final configurations of PET, PLA, and PS in decanoic acid:menthol (1:1). (d) and (e) display the oxygen-hydrogen RDF between PET and PLA respectively with decanoic acid. (f) displays the carbon-hydrogen RDF between PS and decanoic acid. (g) and (h) display the oxygen-hydrogen RDF between PET and PLA respectively with menthol. (i) displays the carbon-hydrogen RDF between PS and menthol. The colors of the lines and legend represent the coordinating atom listed in Figure 28 in APPENDIX 3. (This figure was provided by Qi Qiao and represents results from her simulations.)..... 55

CHAPTER 1. INTRODUCTION

1.1 Plastics

In the 1940s the mass production of synthetic plastic polymers began, and the rate of production has increased rapidly each decade since (Mattsson, Jovic et al. 2018). Plastics have become a vital part of daily life for both consumers and industries due to their strength, stability, durability, and low cost to produce (Sinha, Patel et al. 2010). The benefits of plastic can be seen in improved consumer health and product durability, as well as lowering CO₂ emissions with lightweight materials (Erni-Cassola, Zadjelovic et al. 2019). However, the plastics produced on a massive scale are typically resistant to environmental degradation, causing plastic waste to accumulate in landfills and act as a major pollutant in the ocean (Sinha, Patel et al. 2010). The majority of plastic waste in the ocean comes from land-based sources with material lost by professional and recreation fishing and commercial debris as a secondary source (Avio, Gorbi et al. 2017).

1.1.1 Macro-, Micro-, and Nano-Plastic Particles

Plastic waste in a marine environment can be placed into one of three categories, depending on its size. Large pieces of plastic or anything greater than five millimeters in average diameter are referred to as macro-plastics (Erni-Cassola, Zadjelovic et al. 2019). This category of plastic waste is visible with the naked eye and is the type of plastic that most people are familiar with. Plastic that finds its way into the marine environment will gradually start to break apart into smaller pieces through UV degradation, causing it to become more brittle, and the physical buffeting from the waves. Once the plastic has reached an average diameter of less than five millimeters, it falls into the category of micro-plastic. Upon further degradation to an average diameter of less than 1000

nanometers, the particles are classified as nano-plastic (Erni-Cassola, Zadjelovic et al. 2019). The majority of micro- and nano-plastic polluting the ocean and freshwater comes from the degradation of larger plastic particles, but a portion are synthetic fiber fragments from washing clothes or are manufactured at these sizes as microbeads used in cosmetics and cleaning agents (Wu, Yang et al. 2017).

1.1.2 Environmental and Ecological Impacts

As reports of the increasing numbers of micro- and nano-plastic in the environment have gained attention, various studies looking at the ecological harm caused by these particles have been conducted.

Micro- and nano-plastic particles can be ingested by a diverse range of marine fauna and can consequentially enter the human food chain. At the bottom of the ocean's food chain are phytoplankton and zooplankton which may ingest microplastics floating on or near the surface. These organisms can then indirectly introduce plastic particles into animals that humans will consume (Figure 1). Even without ingesting these particles, microplastics may substitute the normal feed of small organisms, limiting the potential energy within their populations and affecting an important part of the marine ecosystem (Wu, Yang et al. 2017).

When ingested, micro-plastics have been reported to cause inflammation and even damage at the cellular level (Reimonn, Lu et al. 2019). One of the major potential threats these particles pose is the adsorption of toxic or harmful chemicals on their surface. Due to the hydrophobicity of their surfaces, micro- and nano-plastic particles have the potential to adsorb and concentrate toxic hydrophobic substances that are already present pollutants in the environment. These contaminants could be pesticides, flame retardants,

or polychlorinated biphenyls (Wu, Yang et al. 2017). Bio-membranes or eco-corona colonies can accumulate on the surface causing the particles to be more susceptible to adsorbing harmful chemicals (Reimonn, Lu et al. 2019). These particles can then be transported long distances through ocean currents, effectively spreading these contaminants over a larger area (Wu, Yang et al. 2017, Peng, Chen et al. 2018, Nguyen, Claveau-Mallet et al. 2019, Reimonn, Lu et al. 2019). As these particles degrade and separate into more nano-particles, the surface area to volume of plastic particles increases causing more potential adsorption on their surfaces (Reimonn, Lu et al. 2019). At the nano scale, these particles can interact with biological surfaces and molecules differently, causing altered interactions and potentially penetrating membranes (Mattsson, Jovic et al. 2018). Studies suggest that plastic pollution in the marine environment does pose a real threat to organisms at a molecular level (Avio, Gorbi et al. 2017).

Plastic particles are complex mixtures of chemicals and compounds of polymeric substances, production byproducts, and chemical additives. Over time, broken polymer chains can enter the external environment. Toxic byproducts, like BPA and phthalates, used in production may still be present in the plastic and can leach into the environment. Some additives used to enrich the quality of the plastic may be toxic (Reimonn, Lu et al. 2019).

These problems are exaggerated by the inert characteristics and long degradation times of plastics, causing plastic already present in the ocean to continue to cause issues over an extended period of time (Avio, Gorbi et al. 2017).

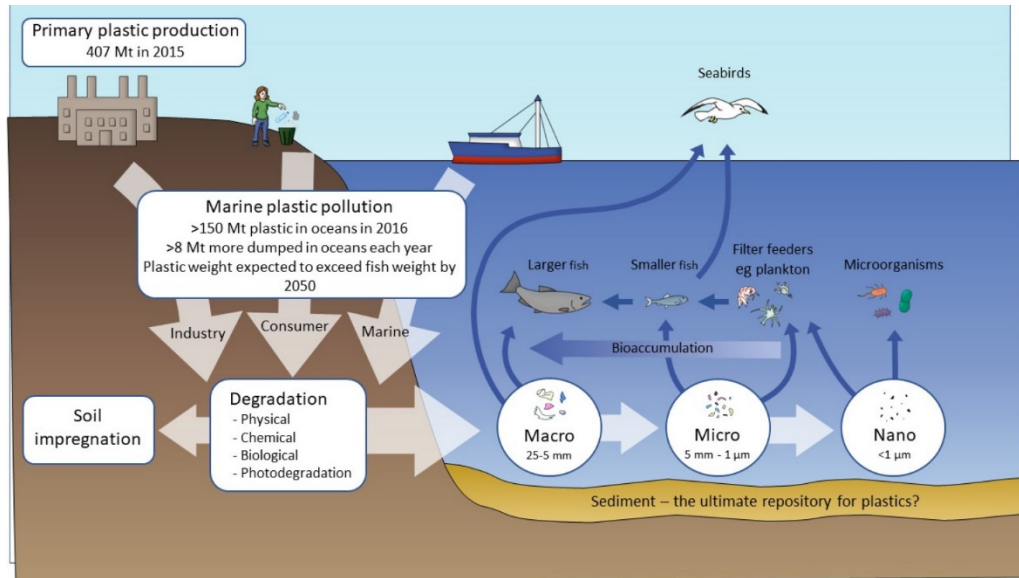


Figure 1 Flow chart of how plastic enters the environment and ecosystem
(Gangadoo, Owen et al. 2020)

1.1.3 Pollution Numbers

In 2015 global plastic production exceeded 300 million tons, with polyethylene terephthalate accounting for 6.9% and polystyrene for 7.1% (Wu, Yang et al. 2017). The majority of plastic products are designed for single use packaging or consumer products, and only eighteen percent of overall plastic wastes have been recycled, and even less incinerated (Jem and Tan 2020). It is estimated that over eight million tons of plastic enter the oceans annually (Erni-Cassola, Zadjelovic et al. 2019). Roughly 100 to 200 million tons of plastic was already present in the ocean in 2020. At the rate plastic is entering the ocean, the mass of plastic will overtake the mass of fish by the year 2050 (Jem and Tan 2020). Concentration of microplastics range from 2.06 to 13.51 pieces per liter with the higher range being comparable to the microplastic concentrations found in coastal waters that are considered to be highly polluted (Peng, Chen et al. 2018).

Plastic is found in all major oceanic currents, polar seas, and deep-sea sediments (Erni-Cassola, Zadjelovic et al. 2019). Microplastic particles have been found in samples from 1000 to more than 5000 meters deep in the ocean, in the Great Lakes of the United States, and in sediment samples from the river Rhine in Germany (Reimonn, Lu et al. 2019). Most plastics found in freshwater are under five millimeters in average diameter and fall into the microplastic category. Plastic constitutes between sixty and eighty percent of total debris in the marine environment (Mattsson, Jovic et al. 2018). Polyethylene, polypropylene, polystyrene, and polyphthalamide plastics are among the most common polymer types found in marine environments (Erni-Cassola, Zadjelovic et al. 2019). There has been a push in recent years for more bioplastics, like polylactic acid, that are quicker to biodegrade. In 2019, an estimated 190,000 tons of polylactic acid plastic was produced and this number is likely to increase every year (Jem and Tan 2020).

1.1.4 Collection and Control

With large amounts of plastic discarded every year, researchers have suggested that a priority should be placed on reducing the amount of plastic entering the environment (Wu, Yang et al. 2017). This can be done by removing particularly harmful products, like microbeads in personal care products, and improving the reuse, recycling, and recovery of plastics. The presence of micro- and nano-plastics in the environment is a symptom of a larger recycling problem. By waiting for plastic to reach these particle sizes, society loses out on the relative ease of collection and value of the plastic. For the plastic already present in the environment, the recovery of plastics is vital. However, currently employed recovery and separation techniques for micro- and nano-plastics are

generally inaccurate, time-consuming, or specific only to certain particle sizes (Reimonn, Lu et al. 2019).

Some of the currently employed techniques to separate plastics from contaminated waters are passive density and size separation, but these are not well-suited for particles on the micro or nano scale. Micro- and nano-plastics can have different properties, such as buoyancy and surface charge from larger pieces of the same types of plastic, making these techniques less effective (Nguyen, Claveau-Mallet et al. 2019). Nguyen et al. suggest that techniques from other fields of research could work better for these types of particles (2019). Active density separation, like centrifugation, could be useful in separating plastic types with different densities. Some techniques can take advantage of surface interactions between the particles and a separation serum.

Hydrophobicity-based separation approaches have been applied from the separation of minerals down to the molecular scale to separate biomolecules (Nguyen, Claveau-Mallet et al. 2019). Froth flotation uses bubbles to separate minerals by taking advantage of the hydrophobicity of the particles to adhere to the surface of bubbles which then carry the particles to the air-liquid interface. However, the unpredictability of the bubbles results in varying recovery rates. Other studies have had some success using oils to capture plastics via oleophilic interactions, but this technique would require processing to remove oil residue.

For analytical studies, plastic is often collected from water's surface using neuston nets, but these are only used to collect small samples and would have issues scaling up for larger plastic recovery. A newer technique for recovering microplastics is solvent extraction. Polymers are dissolved in a certain solvent and heated to a designated

temperature where it is then cooled and put into a new non-solvent. Xylene has shown high yields of recovery for most polymers tested (Reimonn, Lu et al. 2019).

Aside from collecting plastic particles, sorting and identifying them has been an issue. Some of the methods used for analytical studies have scalability problems. FTIR and Raman spectroscopy both provide information on functional groups, but Raman has shown more success at identifying particles of smaller than ten micrometers.

Chromatography with mass spectrometry can identify plastics based on the mass to charge ratio giving the elemental/chemical composition for the particles. Thermal analysis provides information on thermal performance of samples with a mixture of plastics and particles made of polymer blends. Recently, research has been done on UV-microscopy to separate polymeric particles from organic matter (Reimonn, Lu et al. 2019).

1.1.5 Polyethylene Terephthalate

Polyethylene terephthalate (PET) is a commonly used petroleum-based plastic polymer for single use drinking bottles, fibers, films, and containers due to its strength and resilience (Figure 2). It is among the six most-produced plastics and is among the most recycled plastics produced, however, the recovery rate of PET is still low and large amounts of PET enter landfills and the ocean annually (Kawai, Kawabata et al. 2020). Its toughness and non-degradable nature cause it to accumulate at a rapid rate when present in the environment. Because of this, there are numerous studies being done on chemically recycling PET to better make use of the large amount already present within the environment (Raheem, Noor et al. 2019).

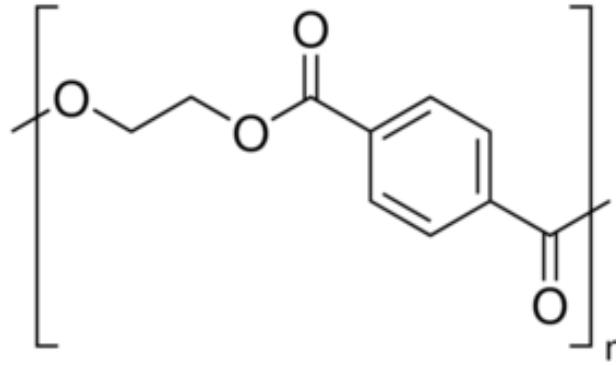


Figure 2 Chemical Structure of Polyethylene Terephthalate

1.1.6 Polystyrene

Polystyrene (PS) is commonly used as insulation for construction, packaging foam, food containers, disposable cups, plates, and cutleries due to its mechanical properties and relatively low cost. PS is another polymer that is among the six most-produced globally and has accumulated in the environment at an alarming rate. PS can be manufactured as either a solid or foam. Solid PS has the potential to be recycled, but foamed PS is not commonly recycled due to its lightweight and bulky nature making the transportation costs too high (Ho, Roberts et al. 2018).

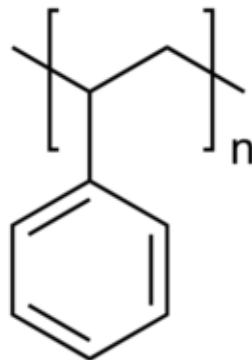


Figure 3 Chemical Structure of Polystyrene

1.1.7 Polylactic Acid

In recent years, bio-based plastics have been developed in an attempt to replace petroleum-based plastics that remain in the environment for extended periods of time. Polylactic acid (PLA) is derived from lactic acid, a renewable resource obtained through fermentation, and is one of the most commercially successful bioplastics developed due to its processability and mechanical properties (Figure 4). Its mechanical strength, durability, and transparency have made it useful in short life-time packaging. PLA is designed to degrade in months at a temperature around 58 °C, which is typical in an industrial composting environment, but does not occur in a marine environment where plastic litter often finds itself (Jem and Tan 2020).

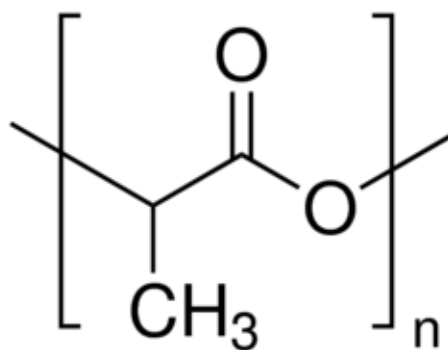


Figure 4 Chemical Structure of Polylactic Acid

Deep eutectic solvents (DES) are a relatively recently discovered solvent formed by a combination of hydrogen bond donors and hydrogen bond acceptors (van Osch, Zubeir et al. 2015). Typically, the individual components are a solid at room temperature, but when mixed have a melting point much lower than either component due to self-

association. The first DES reported were composed of amides and choline chloride, where the components liquified upon contact, most likely due to hydrogen bonding and van der Waals interactions between the components (Van Osch, Dietz et al. 2019).

In recent years, there has been a push for solvents that are less toxic and are made from natural materials. A sub-category of DES called natural deep eutectic solvents (NADES) are made from non-toxic components derived from natural materials, like the monocyclic monoterpenoids menthol and thymol (Van Osch, Dietz et al. 2019). These NADES are generally accepted as environmentally friendly and have the potential to obey the Twelve principles of Green Chemistry set forth by Anastas et al. (2009). Green Chemistry is the design of chemical products and processes to reduce or eliminate the use and generation of hazardous substances. The twelve principles are a guiding framework that include the prevention of waste, designing safer chemicals, using renewable feedstocks, and designing for degradation (Anastas and Warner 1998). Many of the NADES discovered so far have followed these guidelines and new NADES are being discovered regularly.

DES have gained attention in recent years for their similar properties to ionic liquids (van Osch, Zubeir et al. 2015). DES have low volatility, a wide liquid range, are water-compatible, are non-flammable, and they are typically biocompatible. While NADES are generally considered non-toxic and biodegradable, they are still relatively new solvents, and more studies need to be conducted to confirm these statements. Two of the largest advantages of DES over ionic liquids is in the lower cost of components and the ease of preparation. To make DES, a molar ratio of two solid components only need

to be mixed at a slightly elevated temperature with no need for a purification step (van Osch, Zubeir et al. 2015).

The properties of a given DES are affected by the selection of components in regards to molecular structure, chemical nature, ratio, and water content (van Osch, Zubeir et al. 2015, Liu, Friesen et al. 2018). The majority of DES discovered have been hydrophilic in nature, but discoveries of hydrophobic varieties have been reported. For example, decanoic acid is an amphipathic molecule that can act as a hydrogen bond acceptor and donor. Liu et al. have reported a broad polarity range for NADES media (2018).

1.1.9 Recent Development in DES and Application in Compound Extraction

Van Osch et al. report the first hydrophobic deep eutectic solvents consisting of a fatty acid and a quaternary ammonium salt. The leaching of the hydrogen bond acceptor, ammonium salts, into water depends on its carbon chain length. As alkyl chain lengths increased, the DESs showed a trend of increasing viscosities and extraction efficiencies. They also found that salts containing a bromide anion had higher viscosities compared to DES containing a chloride anion. The decomposition temperatures were high, and the hydrophobicity of the DES was determined through the water content, after mixing with water, and low leaching of the quaternary ammonium salts. They concluded that hydrophobic DESs have potential in liquid-liquid extraction processes by testing their ability to extract sulfur compounds from model oil (van Osch, Zubeir et al. 2015).

Van Osch et al. conducted a search for natural hydrophobic deep eutectic solvents by mixing different terpenes (Figure 5) together and analyzing the results against a set of

criteria (2019). Three of the hydrophobic NADESs that they found were Decanoic Acid:Menthol at a 1:1 and 1:2 molar ratio and Thymol:Menthol at a 1:1 ratio. After mixing these NADES with water, their water content was found to be 2.1 wt%, 2.07 wt%, and 1.81 wt%, which proves the hydrophobicity of the NADES. They also reported studies where hydrophobic NADESs have been used to remove metal ions, furfural, and hydroxymethylfurfural with membrane technology, and pesticides from water (Van Osch, Dietz et al. 2019).

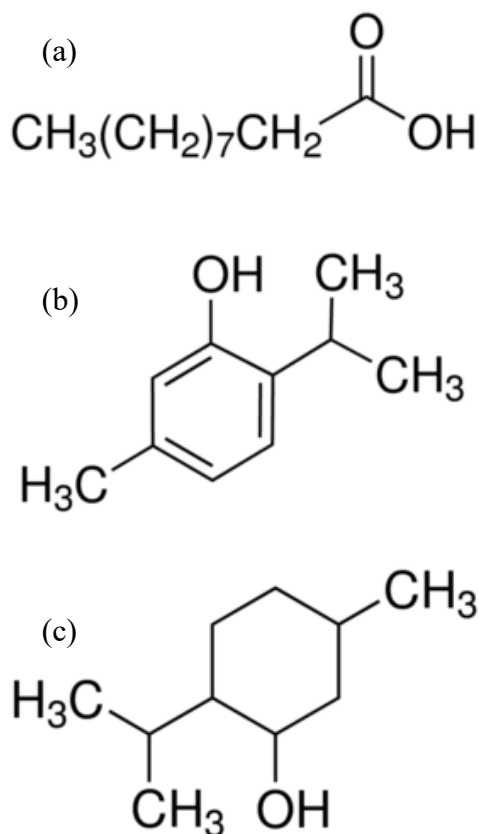


Figure 5 Chemical Structures of (a) Decanoic Acid, (b) Thymol, and (c) Menthol

Cunha et al. reviewed different extraction techniques possible with deep eutectic solvents. One of the more promising techniques was liquid-phase microextraction using

low amounts of sample matrices and small volumes of organic solvents. DES and NADES showed excellent potential as extracting solvents in several sample preparation procedures such as ultrasound assisted microextraction and microwave assisted extraction. This study was focused on microextraction techniques using DES/NADES as extracting solvents for food, biological, and environmental sample analysis. Studies have shown that these solvents have a high potential as extracting solvents for a wide range of analytes. Some of these other analytes were phenolic compounds from virgin olive oil, polycyclic aromatic hydrocarbons from choline chloride-oxalic acid solutions, and antioxidant flavonoids (Cunha and Fernandes 2018).

Makos et al. focused on hydrophobic NADES as extraction media for polycyclic aromatic hydrocarbons. PAHs are classified as priority environmental pollutants due to their carcinogenic and mutagenic properties, but they are hard to detect in samples of industrial effluents because of their low concentration and complex matrix. The NADES used in this study were based on thymol with camphor and thymol with 10-undecylenic and decanoic acids. Final determination of analytes extracted were carried out by gas chromatography-mass spectrometry. Extraction took place using 10 ml of effluent and 200 μ L of NADES in an ultrasonic bath for 14 min, then centrifuged. It was found that NADES in dispersive liquid-liquid microextraction is an attractive alternative to toxic chlorinated solvents and meets all the requirements of Green Chemistry (Makoś, Przyjazny et al. 2018).

Xu et al. looked at DES as alternatives to ionic liquids in biocatalytic processes. Biocatalysis is defined as reactions catalyzed by biocatalysts, like isolated enzymes and whole cells. Ionic liquids were the first enzyme-compatible untraditional media

developed by the green and sustainable concept. However, despite the good performance of ionic liquids in biocatalysis, there are concerns about their potential effects on the environment. Xu et al. reviewed some of the applications of DES in biocatalysis so far. Studies have found hydrolases exhibited better activity in DES compared to their activity in ionic liquids and hydrolysis and transesterification reactions catalyzed in a number of DES. As solvents, DES can potentially activate and stabilize the enzyme, achieving a high reaction efficiency. Multiple hydrolases (lipase, protease, and epoxide hydrolase) and other enzymes exhibit great catalytic performance in DES. These studies show progress, but Xu et al. concluded that more physical-chemical characterization and toxicity data need to be done on DES in general before they can be fully declared as green solvents (Xu, Zheng et al. 2017).

1.2 Motivations and Objectives

Based on the literature review, micro- and nano-scale plastic particles (nano-plastics) has become the subject of increasing concerns because their small size makes them hard to remediate using traditional separation methods. Hydrophobic NADES is a promising candidate for extracting organic substrates from the aqueous solutions because they are relatively cheap and less toxic as compared to the other common solvents. However, to the best of our knowledge, hydrophobic NADES has not been investigated for micro- and nano-plastics extraction.

The overarching goal of this project is to investigate the relationship between the hydrophobic natural deep eutectic solvents decanoic acid:menthol (1:1), decanoic acid:menthol (1:2), and thymol:menthol (1:1), with nano-particles of the synthetic

polymers polyethylene terephthalate, polystyrene, and polylactic acid, in a liquid-liquid extraction system.

The objectives of this work are to synthesize and characterize the hydrophobic natural deep eutectic solvents, develop a method for synthesizing and characterizing plastic nano-particles, and measuring the quantity of particles extracted from an aqueous phase by the hydrophobic NADES over an extended period of time. Through a collaboration with chemical and material engineering department, molecule dynamic simulations are carried out to study interactions between plastic and NADES molecules. Collectively, this research can help rationalize the design of hydrophobic NADESs and spur the development of processes to remediate plastics from aqueous systems.

CHAPTER 2. MATERIALS AND METHODS

2.1 Materials

2.1.1 Chemicals

The materials for the deep eutectic solvents and plastics were purchased online through Sigma-Aldrich and VWR. $\geq 98\%$ Decanoic acid, 99% menthol, $\geq 99\%$ thymol, and granular polyethylene terephthalate reinforced with glass were purchased through Sigma-Aldrich. Polystyrene pellets were purchased from Acros Organics. Granular polylactic acid was purchased from GoodFellow Cambridge Limited. Chemicals used in the preparation of the plastic particles were $\geq 99\%$ phenol, $\geq 99\%$ *p*-xylene, and $>99\%$ ethanol, which were all purchased from Sigma-Aldrich. $\geq 99\%$ Acetonitrile was purchased from VWR. Deionized water used as needed was filtered by the Barnstead NANOpure ultrapure water system. Films of polyethylene terephthalate and polystyrene were purchased from GoodFellow (Coraopolis, PA).

2.1.2 Equipment

General laboratory equipment like beakers, kimwipes, pipettors, pipette tips, and falcon tubes were purchased through VWR. Glass vials used in experiments were 4.5 cm tall and 1.4cm in diameter. Spectrophotometer plates were Thermo Scientific 384 well plate clear. Stir bars used were SpinFin 8mm diameter by 9.5 mm height and SpinFin 9.5 mm diameter by 9.5 mm height from SP ScienceWare. Disposable Pasteur pipets were purchased through Fisherbrand. Other equipment used were the accu-jet® pro electric pipettor, VWR vortex mixers, VWR hot plate stirrer, Heidolph MR Hei-End magnetic hot plate stirrer, Heidolph MR Hei-Tec magnetic hot plate stirrer, Branson 2800

bath sonicator, the Marathon 21000 centrifuge from Fisher-Scientific, Labconco FreeZone freeze dryer, and VWR vacuum oven. Analytic equipment used were the Molecular Devices SpectraMax M2 spectrophotometer, Malvern Panalytic Zetasizer Nano ZS for dynamic light scattering and zeta potential, and the Krüss Drop Shape Analyzer for contact angle measurements.

2.2 NADES Synthesis

To synthesize the deep eutectic solvents, each component was weighed out according to the necessary molar ratio. For this project, a 1:1 and 1:2 molar ratio of decanoic acid:menthol and a 1:1 molar ratio of thymol:menthol were used. The components for each NADES were placed into their own glass vial with a screw on lid and heated at 40 °C with periodic vortexing until the mixture is completely liquid. The synthesized NADES were kept in capped bottles in a desiccator at room temperature until use.

2.3 NADES Characterization

2.3.1 Contact Angle Measurements

Analysis of the hydrophobicity of the deep eutectic solvents was done by measuring the contact angle of a 3 μ L droplet of NADES on films made from the three plastics tested in this project.

Contact angles of the NADES on polyethylene terephthalate and polystyrene were conducted on mechanically manufactured films, but the film of polylactic acid had to be synthesized in the lab. The film was made with a doping solution of 20% polylactic acid

in acetonitrile (w/w) poured on a sheet of clean glass and spread thin. It was left to evaporate for two min then placed in a water bath. The film was then moved to a storage container filled with DI water for one day. Before use, the films were wiped down with paper towels and the remaining DI water was allowed to air dry.

To measure the contact angle, a 4 cm² portion of one of the plastic films was cut and secured to a glass microscope slide with double-sided tape. It was then washed with ethanol to remove any oils from the surface. A syringe with 3 μ L of NADES is secured on the mechanical arm above the reading platform. The slide is then placed on the reading platform and adjusted so the plastic film is centered under the needle. The arm is lowered until the tip of the needle is visible in the camera and the plunger is pushed so a droplet forms at the tip. Resolution is adjusted to focus the droplet and the arm is lowered until contact is made with the film. The needle is raised and contact angle measurements are taken at zero seconds and every ten seconds for the next minute. Each NADES was measured twice on each plastic film, with the syringe being washed with ethanol between changes in NADES.

2.4 Plastic Particle Preparation

2.4.1 Polyethylene Terephthalate

Polyethylene terephthalate particles were prepared by solubilizing granulated PET in phenol and then precipitating the PET at a small size in ethanol. For this process, 0.1 g of PET and 4 g of phenol were weighed and placed in a capped vial with a magnetic stir bar. This vial was left on a magnetic stir plate set at 80 °C and 250 rpm for two hours until PET was completely solubilized. Using a glass Pasteur pipette, the phenol/PET

mixture was then slowly dripped into a 100 mL sized beaker with 50 mL of ethanol being stirred at 400 rpm. The mixture was transferred into a Falcon tube and centrifuged at 4000 rpm for 10 min. The effluent was placed in a hazardous waste container and the 40 mL of DI water was poured into the Falcon tube and vortexed to wash the particles before being centrifuged again. This washing step was repeated two more times. Because some PET is lost in the washing process, the final concentration was determined by drying 1 mL of the mixture in three pre-weighed vials in a vacuum oven at 60 °C. The average of the difference before and after drying was used to adjust the concentration of PET in the DI water to 1 mg/mL. The mixture was stored at room temperature in a lidded glass container.

2.4.2 Polystyrene

The polystyrene particles were prepared in a similar fashion to the PET particles, 0.1 g of PS pellets and 4 g of ethyl acetate were weighed and placed in a capped vial with a magnetic stir bar. This vial was left on a magnetic stir plate set at 40 °C and 500 rpm for 2 h until the PS was completely solubilized. The PS particles then went through the same steps as the PET particles for precipitation, washing, and adjustment of concentration.

2.4.3 Polylactic Acid

The polylactic acid particles were prepared similarly to the PET and PS particles, 0.1 g of PLA pellets and 4 g of acetonitrile were weighed and placed in a capped vial with a magnetic stir bar. This vial was left on a magnetic stir plate set at 40 °C and 500 rpm for 2 h until the PLA was completely solubilized. The PLA particles then went

through the same steps as the PET and PS particles for precipitation, washing, and adjustment of concentration.

2.5 Particle Size Distribution and Zeta-Potential Analysis

Particle size distribution and zeta-potential for each plastic type was conducted using dynamic light scattering on a Malvern Panalytic Zetasizer Nano ZS. Each plastic sample was diluted to 0.05 mg/mL and vortexed before reading. Each sample was measured three times.

2.6 Plastic Particle Extraction

2.6.1 Determining Plastic Concentration with Optical Density Measurements

To correlate measurements from optical density (OD) measurements, a series of dilutions for each plastic type were made from 0.05 mg/mL to 1 mg/mL and measured along with DI water with no particles in the spectrophotometer at a wavelength of 400 nm.

2.6.2 Polyethylene Terephthalate Extraction

PET extraction experiments were conducted by pipetting 1.75 mL of 1 mg/mL concentration PET in DI water and 0.25 mL of DI water in three 4.5mL volume glass vials. An 8 mm diameter SpinFin stir bar was placed in each vial and they were stirred on a magnetic stirrer at 500 rpm for a few minutes. A 40 μ L sample was taken from each vial and pipetted into a well in a clear 384 well plate. Two mL of one type of NADES were slowly pipetted into each vial so as not to mix the NADES and water phases. A 40

μL sample of the water phase is taken with a 100 μL capacity pipettor by moving the tip through the NADES phase and into the water. After removing the pipette tip from the NADES, the outside of the tip is wiped with a Kimwipe to prevent NADES on the tip from entering the plate well. The initial samples are placed in a spectrophotometer for OD readings at 400 nm wavelength. Each vial is then capped and placed on a magnetic stirrer set at 500 rpm at room temperature (21 °C). A 40 μL sample is taken from each vial every 2 h for the first 8 h. Another 40 μL sample is taken at the 24-, 28-, and 32-h marks. OD readings for each sample are done immediately after samples are taken. This procedure was then repeated for the other NADES.

2.6.3 Extraction of Plastic Particles

PS extraction was conducted similarly to the PET extraction, but the timeframe was extended slightly due to slower extraction rates.

The setup for the PLA extractions were conducted similarly to PET and PS, but the timeframe was significantly reduced due to much faster rates of extraction. For the PLA experiments, a 40 μL sample was taken from each vial every 20 min for the first 2 h, then another sample taken at the 3- and 5-h marks.

2.6.4 Salt-water Extraction

Extraction of the plastic particles in salt-water was conducted by pipetting 1.75 mL of a 1 mg/mL concentration of plastic particles in DI water and 0.25 mL of 28% sodium chloride in DI water in three 4.5 mL volume glass vials. The final concentration of sodium chloride in the water phase will be 3.5% which approximates the salt concentration in seawater. An 8 mm diameter SpinFin stir bar was placed in each vial and

they were stirred on a magnetic stirrer at 500 rpm for a few min. Due to aggregation of the particles, larger samples were taken at 200 μL for the initial concentration readings then replaced into the system. Two mL of NADES were slowly pipetted into the top of the vial and set to stir at 500 rpm.

2.7 Molecular Interaction Simulations

Simulations of interactions between the plastic molecules and NADES/water were conducted by Drs. Qi Qiao and Qing Shao in the chemical and materials engineering department at UK. This section contains a summary of the method; a more detailed methodology is included in APPENDIX 2.

The plastic molecules and NADES were described using the all-atom model and water molecules were described using the TIP 4P model (Jorgensen, Chandrasekhar et al. 1983). Bonded and nonbonded interactions within the system were determined using OPLSAA/M force field (Robertson, Tirado-Rives et al. 2015) which can describe the behavior of organic molecules, and its parameters were assigned using the Ligpargen web server (Jorgensen and Tirado-Rives 2005, Dodda, Cabeza de Vaca et al. 2017, Dodda, Vilseck et al. 2017).

The simulation systems were created within a cubic box with one plastic molecule and a specific number of solvent molecules, which are specified in Table 54 in APPENDIX 2. The simulation program was GROMACS and the system was created using the insert-molecule and solvate tools (Abraham, Murtola et al. 2015). The bonded and nonbonded interactions in the system were determined using the OPLSAA/M force field (Robertson, Tirado-Rives et al. 2015).

2.8 Statistical Analysis and Regression

Statistical analysis of extraction and contact angle data was conducted using the data analysis tool in Microsoft Excel. Regression analysis of extraction data was conducted in SigmaPlot 14.0.

Statistical analysis of the initial rate of extraction and the endpoint of extraction between the plastics in each NADES and each NADES across the different plastics were conducted. An analysis of variance (ANOVA) with a significance level of 0.05 were conducted with the null hypothesis that all the means were equal. A P-value greater than 0.05 would indicate a rejection of the null hypothesis and conclude at least one of the means is significantly different to the others. In the case where the null hypothesis is rejected, two-sample, two-tail t-tests assuming unequal variances were conducted between each mean to determine which means are significantly different from each other.

2.8.1 Polymers across NADES

For each polymer, an ANOVA was conducted with a 0.05 significance level with the NADES as the changing variable for the initial rate and the endpoint.

2.8.2 NADES across Polymers

For each NADES, an ANOVA was conducted with a 0.05 significance level with the polymer as the changing variable for at the 2-h mark and the endpoint. Although, the PLA was measured in a shorter timeframe, the 2-h mark was used to better compare the NADES across the polymers.

CHAPTER 3. RESULTS AND DISCUSSION

3.1 Contact Angle Analysis

The contact angles of the three NADES mixtures were measured on a film of each of the plastics (Table 1, Figure 6, Figure 7, Figure 8). The films made of PET and PS were manufactured commercially, but the PLA film had to be synthesized in the lab. Films created in the lab will not have as smooth or consistent of a surface as the manufactured ones. Because of this, the results from the PLA can show differences between the NADES, but they should not be compared to the results from the PET and PS.

A surface is generally considered hydrophobic if the static water contact angle is greater than 90° and hydrophilic when the contact angle is less than 90° . When measuring the contact angle of a substance other than water on a surface, a contact angle less than 90° suggests an affinity to the surface.

The measured contact of a droplet of water on the PET was close to 80° , which suggests it is slightly hydrophilic. The contact angle on PS and PLA were close to 90° suggesting it is slightly hydrophilic and close to being neutral. For the PLA, the contact angle of the water droplet was slightly above 90° , suggesting a slight hydrophobicity, but due to the film being synthesized in the lab, this result could be affected by its rougher surface.

The contact angles for each of the NADES on the plastic films showed a contact angle less than 90° , suggesting an affinity between them. For the PET and PS films, the NADES would spread upon contact with films. This can be seen in the decreasing values

between the initial measurement at 0 s and 30 s. For the PET film, the two decanoic acid:menthol NADES showed a similar affinity, while the thymol:menthol (1:1) had slightly higher contact angles. On the PS film, the decanoic acid:menthol (1:2) NADES showed the strongest affinity, while decanoic acid:menthol (1:1) and thymol:menthol (1:1) had similar results. Between the two plastics, each of the NADES had a smaller contact angle on the PET film than they did on the PS. The contact angles on the PLA film synthesized in the lab were higher than the those on the other two films, but these could be attributed to a rougher surface or abnormalities in the thickness of the film. For these contact angles, it can be noted that all the NADES had contact angles less than 90 degrees and the two decanoic acid:menthol NADES showed spreading after initial contact, while the thymol:menthol (1:1) did not spread.

Table 1 Contact angle measurements in degrees

	Measurement	PET		PS		PLA	
		0 s	30 s	0 s	30 s	0 s	30 s
Water	1	79.9	81.3	88.3	87.7	92.07	90.23
Decanoic Acid:Menthol (1:1)	1	9.8	<5	22.08	12.83	22.5	22.09
	2	10.04	<5	25.93	9.81	33.19	20.77
Decanoic Acid:Menthol (1:2)	1	9.79	<5	15.46	<5	30.09	23.88
	2	11.9	<5	15.5	<5	28.36	23.17
Thymol:Menthol (1:1)	1	15.05	7.41	19.66	6.95	27.96	27.78
	2	13.71	<5	24.11	7.8	29.73	29.58

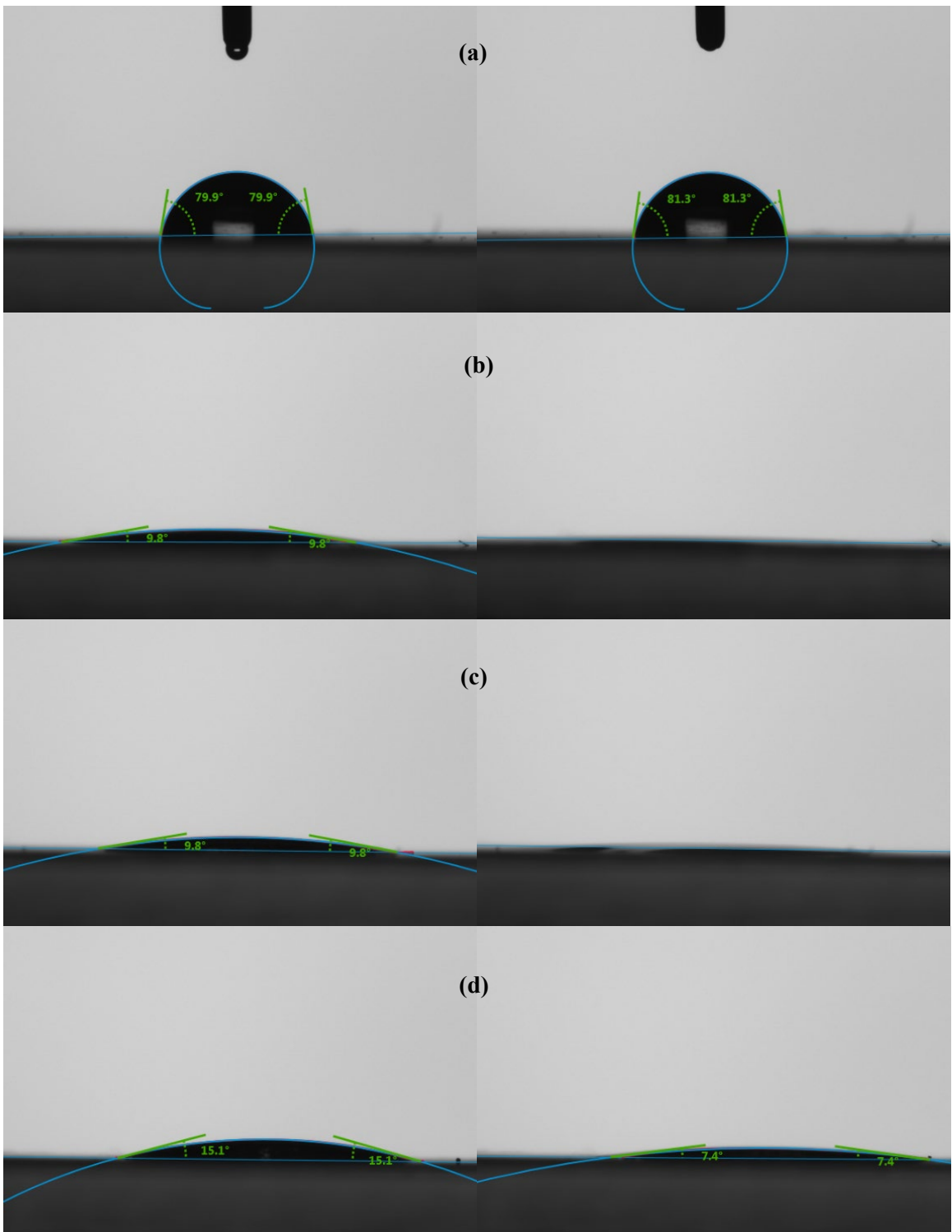


Figure 6 Contact angles of **a)** water, **b)** decanoic acid:menthol (1:1), **c)** decanoic acid:menthol (1:2), and **d)** thymol:menthol (1:1) at 0 seconds (left) and 30 seconds (right) on PET surface.

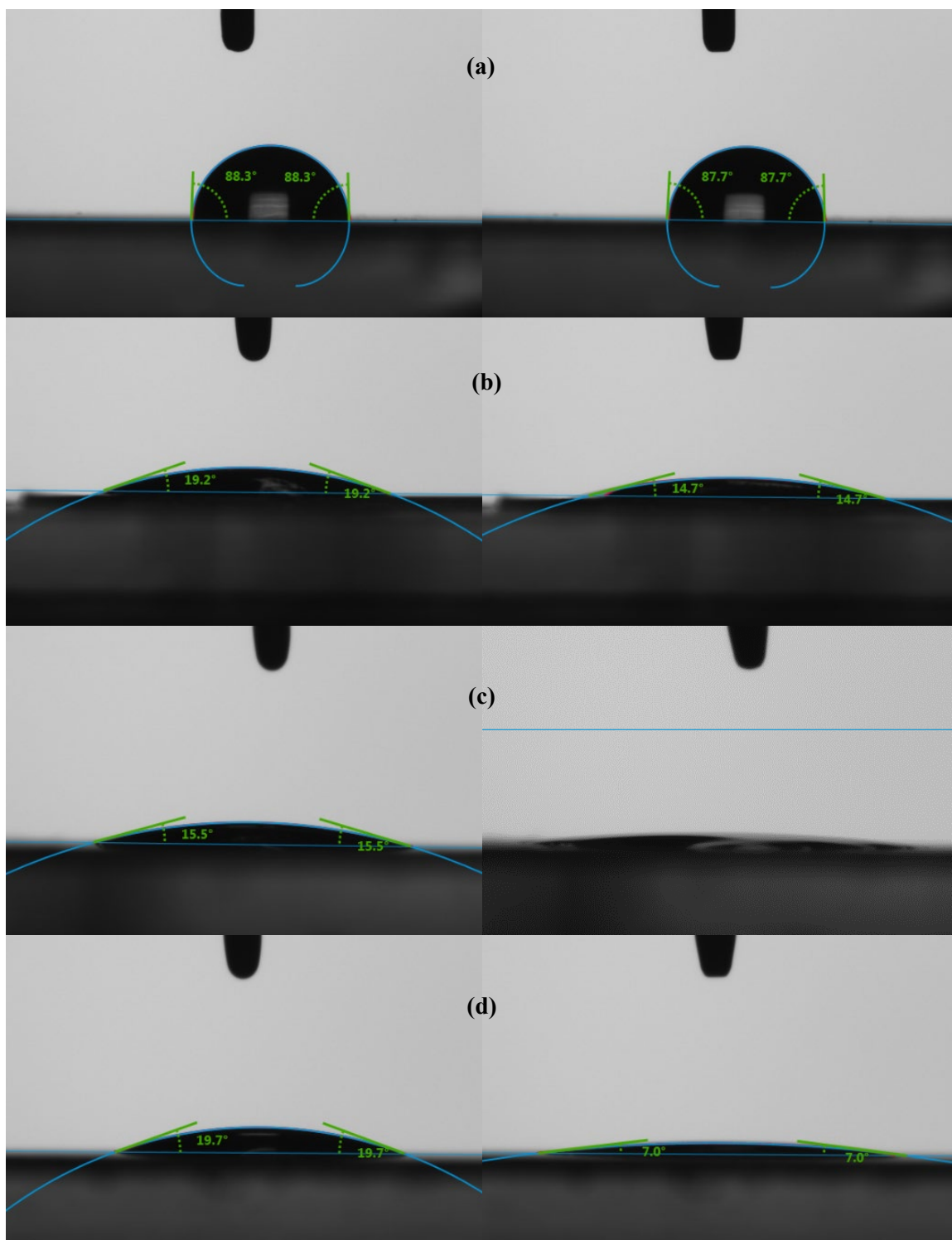


Figure 7 Contact angles of **a)** water, **b)** decanoic acid:menthol (1:1), **c)** decanoic acid:menthol (1:2), and **d)** thymol:menthol (1:1) at 0 seconds (left) and 30 seconds (right) on PS surface.

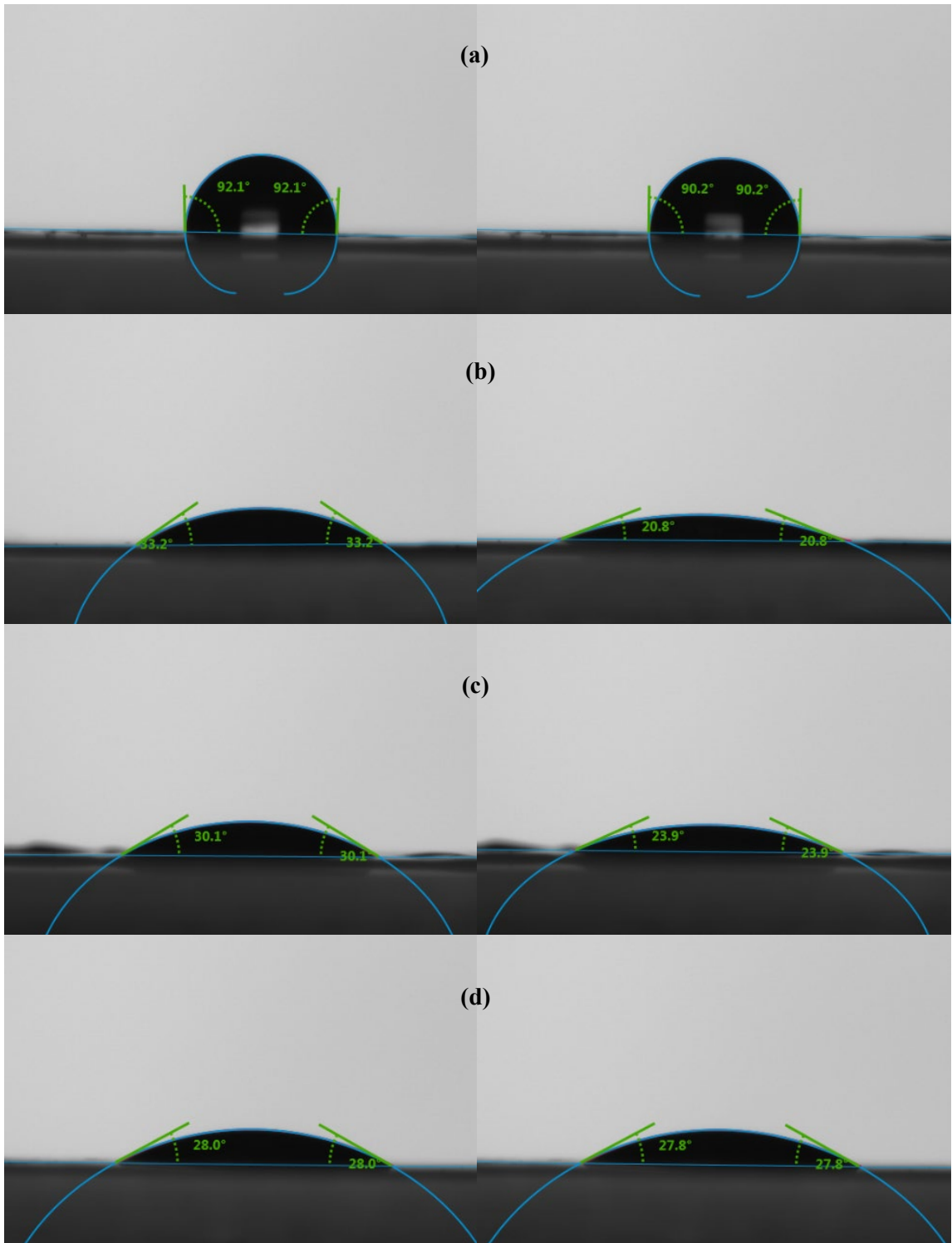


Figure 8 Contact angles of **a)** water, **b)** decanoic acid:menthol (1:1), **c)** decanoic acid:menthol (1:2), and **d)** thymol:menthol (1:1) at 0 seconds (left) and 30 seconds (right) on PLA surface.

3.2 Particle Size Analysis

The size of particles synthesized in DI water was done using dynamic light scattering with three measurements taken for each sample. Z-average is a measurement of cumulant size within a sample and polydispersity index (PDI) measures the how disperse the particles are within the media, the closer to zero the PDI is the more uniform a sample is. The machine used for DLS was also used to measure the zeta potential of the particles, which is the potential difference between the dispersion medium and the stationary layer surround the particles. Typically, the further from zero the zeta potential is, the more stable the suspension of the particles in the medium is.

Each of the plastic particles had an average size less than 1000 nm, classifying them as nano-plastics. The particles followed a trend in size, uniformity, and suspension stability. PS particles were the smallest, most uniform, and stable suspension, followed by PET, and then PLA. The average measurement values with standard error are listed in Table 2.

The z-average gives a number for the average size within each sample, but there is a larger distribution of sizes within the sample. The size distribution and intensity of these particles are represented in Figure 9.

Table 2 DLS measurements in DI water with standard error

	Z-average (nm)	PDI	Zeta potential (mV)
PET	333.6 ± 2.66	0.234 ± 0.0158	-24.7 ± 0.28
PS	263.2 ± 0.84	0.199 ± 0.0145	-29.4 ± 1.37
PLA	774.9 ± 16.40	0.464 ± 0.0335	-19.3 ± 1.23

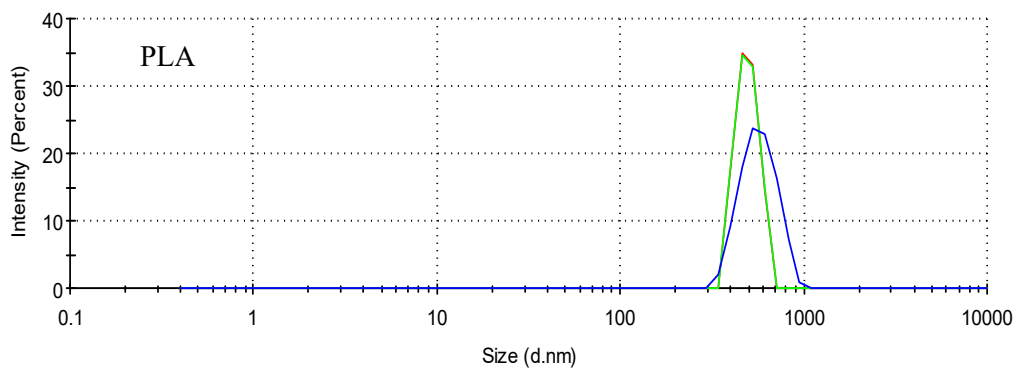
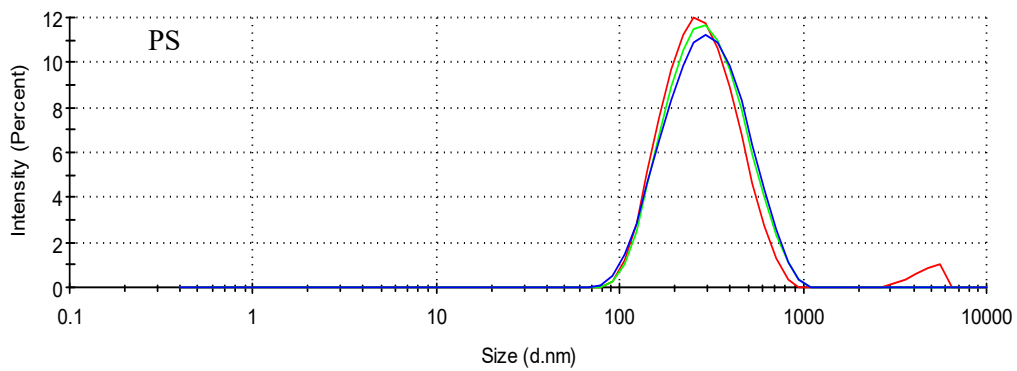
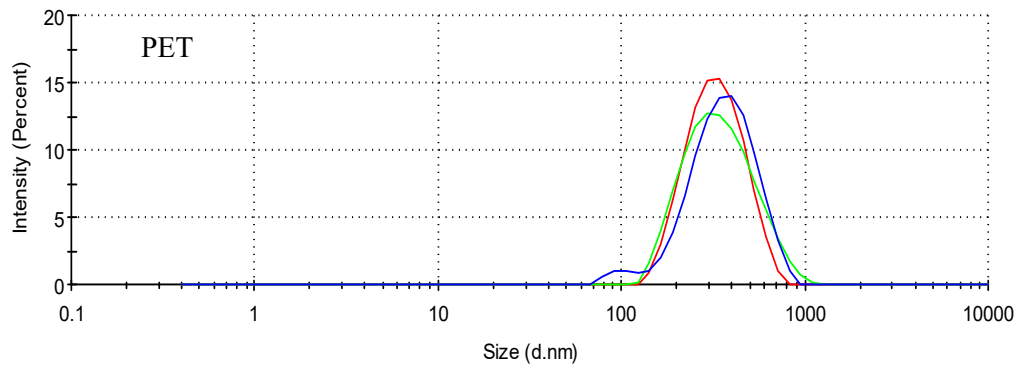


Figure 9 Size distributions of plastic particles (PET, PS, and PLA) in DI water.

The size of the particles in 3.5% sodium chloride in DI water was also measured (Table 3, Figure 10). The particles typically aggregated in the salt-water solution, which is likely due to a change in the zeta potential.

The size and zeta potential followed the same trend as the DI water measurements, but the PDI varied with PET being much less uniform than the other particles which had similar values.

Table 3 DLS measurements in salt-water with standard error

	Z-average (nm)	PDI	Zeta potential (mV)
PET	3870 ± 476.1	0.923 ± 0.0770	-10.9 ± 3.04
PS	3087 ± 254.4	0.351 ± 0.0609	-15.8 ± 1.67
PLA	5769 ± 442.9	0.335 ± 0.0273	7.01 ± 1.398

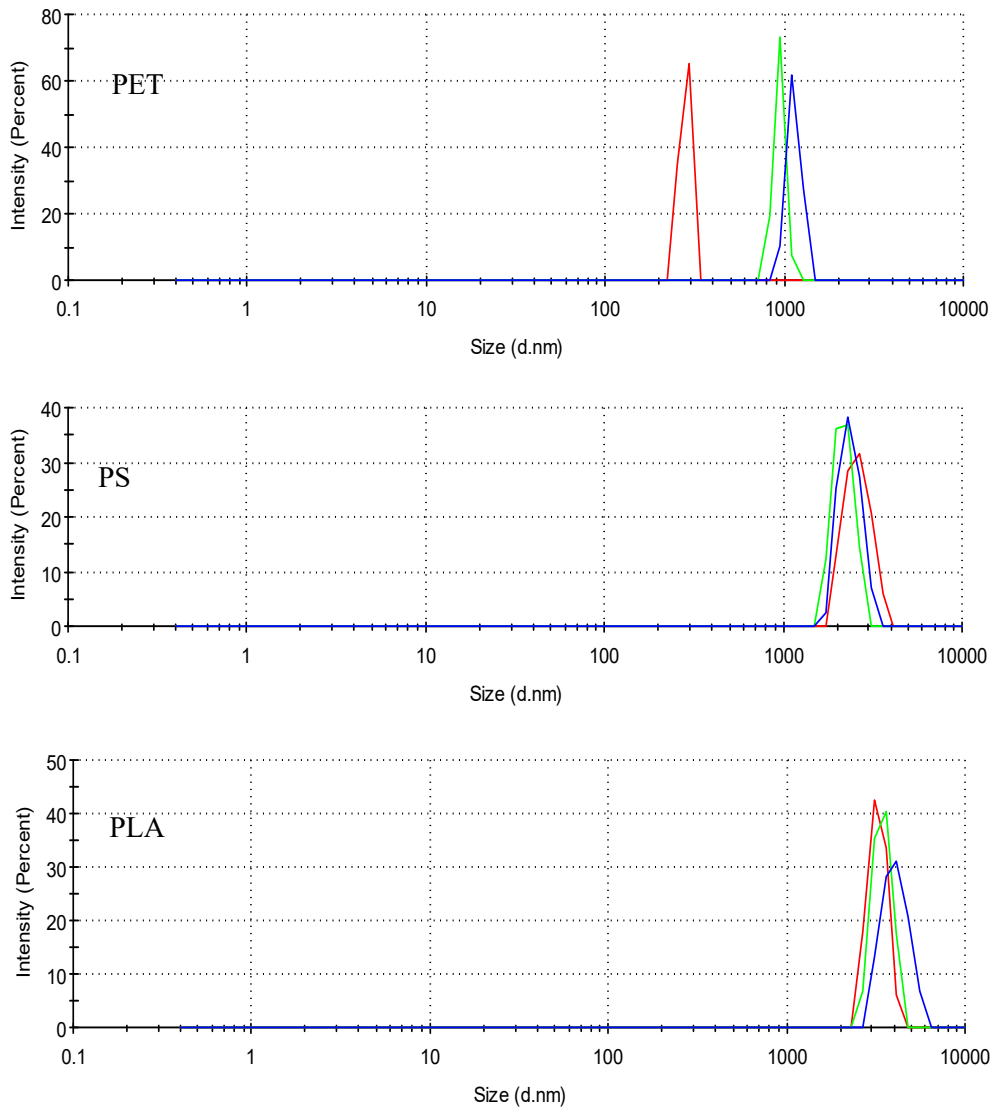


Figure 10 Size distribution for plastic particles (PET, PS, and PLA) in salt-water.

3.3 Plastic Extraction

3.3.1 Concentration of Plastic Particles from Optical Density

Optical density measurements at 400 nm were taken at concentrations of each plastic to determine a correlation between concentration of plastic particles in the sample and absorbance values.

Absorbance values for PET and PLA showed a linear correlation with concentration values ranging from 0 to 1 mg/mL of plastic particles (Figure 11 and Figure 13). PS had optical density readings between 1 and 2 which lie outside of the linear range of the spectrophotometer (Figure 12). A 2nd order polynomial trend with an R^2 value of 0.9996 was used to coordinate the readings with concentrations as most of the OD measurements would likely be between 0 and 1 where the machine is the most accurate.

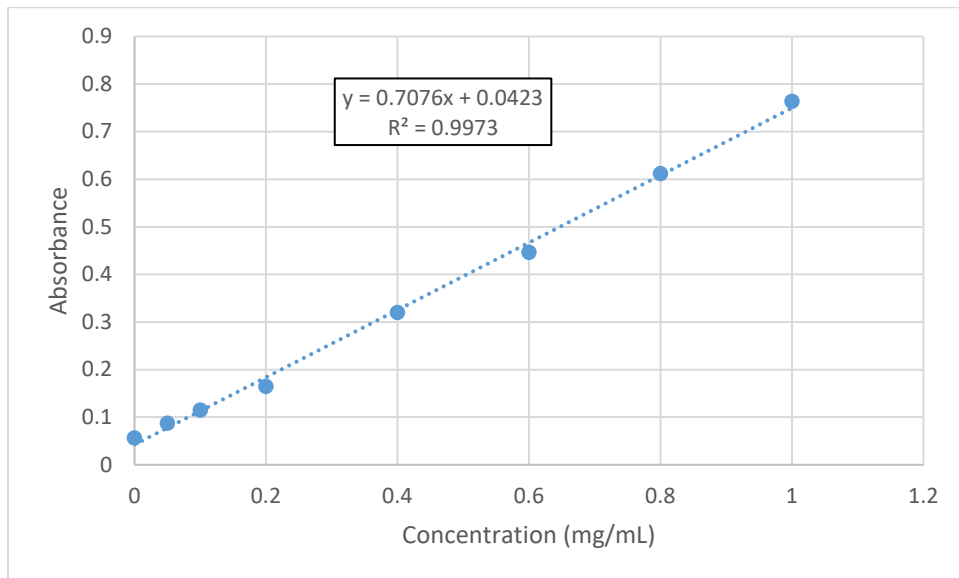


Figure 11 PET Concentration vs Absorbance Correlation

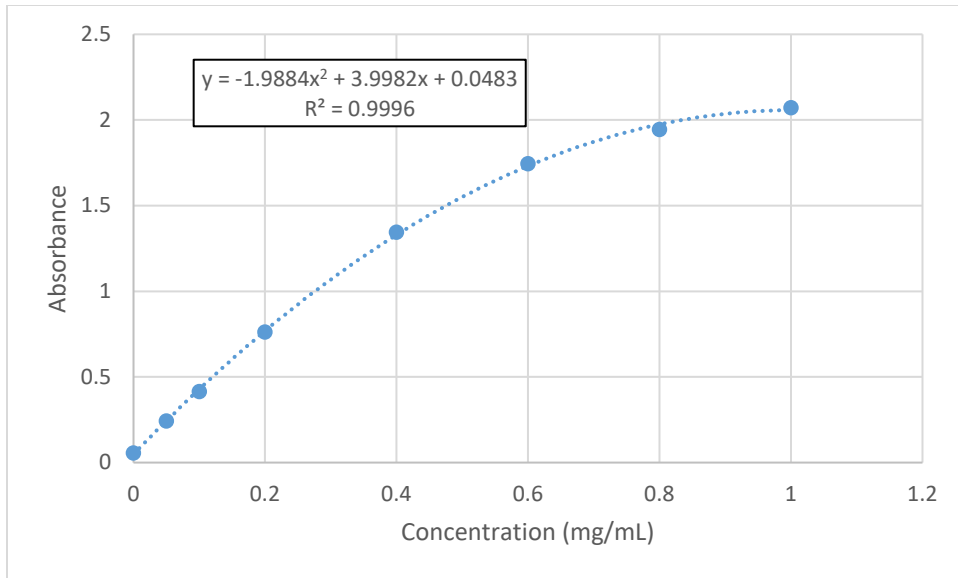


Figure 12 PS Concentration vs Absorbance Correlation

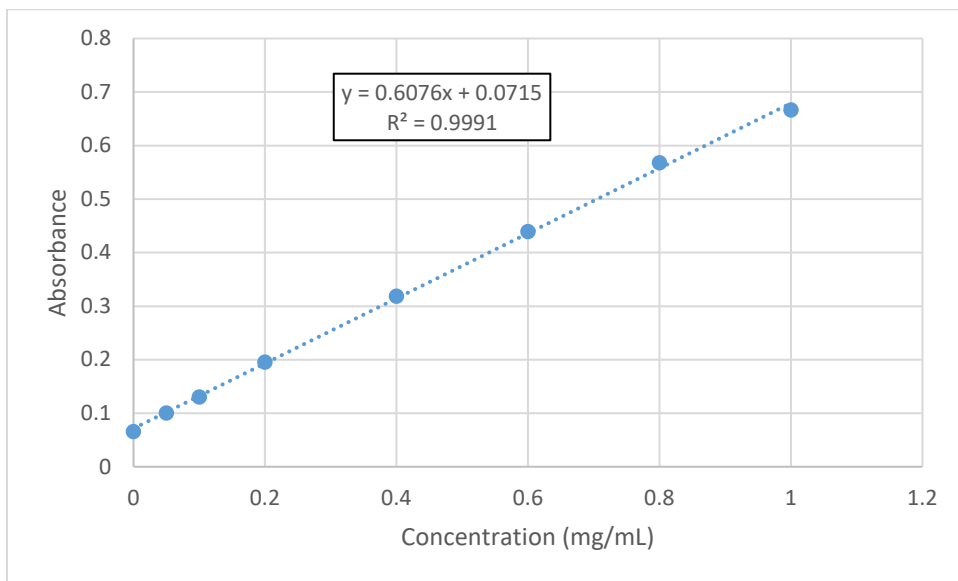


Figure 13 PLA Concentration vs Absorbance Correlation

3.3.2 PET Extraction

The extraction of PET particles took place over a 32-hour period, and the percent of particles extracted forms an isotherm shaped curve when plotted against time. Table 4 shows the percent of PET extracted from each sample after 2 and 32 h.

Table 4 PET Extraction Percent at 2 h and the endpoint

	2 h		Endpoint (32 h)	
	Mean	St. Error	Mean	St. Error
Decanoic Acid:Menthol (1:1)	58.6%	6.00%	77.5%	2.02%
Decanoic Acid:Menthol (1:2)	54.9%	4.12%	70.8%	1.57%
Thymol:Menthol (1:1)	47.7%	7.13%	75.0%	4.89%

In comparing the three NADES, decanoic acid:menthol (1:1) reached an equilibrium at an average extraction of 77.5%, decanoic acid:menthol (1:2) reached an equilibrium at an average extraction of 70.8%, and thymol:menthol (1:1) reached an equilibrium at an average extraction of 75%.

3.3.3 PS Extraction

The extraction of PS particles took place over a 32-h period like the PET extraction, but due to a slower extraction rate more samples were taken at later time points as well. The percent of particles extracted forms an isotherm shaped curve when plotted against time. Table 5 shows the percent of PS extracted with standard error from each sample after 2 h and at their endpoints.

Table 5 PS Extraction Percent at 2 hours and the endpoint

	2 h		Endpoint	
	Mean	St. Error	Mean	St. Error
Decanoic Acid:Menthol (1:1)	50.3%	5.01%	71.5%	3.70%
Decanoic Acid:Menthol (1:2)	10.5%	4.72%	70.0%	2.73%
Thymol:Menthol (1:1)	40.5%	9.67%	60.3%	7.77%

Decanoic acid:menthol (1:2) did not reach equilibrium within the 32-h period and showed significant increases in extraction after the extended time period. At 48 h the percent extracted was 67%, 67%, and 54%, and after 96 h the percent extracted was 74%, 70%, and 65%. This suggests a significantly slower extraction rate and would reach a

similar equilibrium to decanoic acid:menthol (1:1), but we cannot state what the equilibrium for this NADES is because more samples were not taken after the 96-h mark. Thymol:menthol (1:1) showed consistency in extraction rate but had wide range in the point of equilibrium. There was no significant change in percent extracted after taking samples the next day.

3.3.4 PLA Extraction

The extraction of PLA particles took place over a 5-h period due to a significantly higher extraction rate than the other two plastic particles. The percent of particles extracted forms an isotherm shaped curve when plotted against time. Table 6 shows the percent of PLA extracted with standard error from each sample after 20 min and 5 hours.

Table 6 PLA Extraction Percent at 20 min and the endpoint

	20 min		Endpoint (5 h)	
	Mean	St. Error	Mean	St. Error
Decanoic Acid:Menthol (1:1)	51.3%	5.80%	83.4%	5.76%
Decanoic Acid:Menthol (1:2)	47.1%	0.45%	78.1%	2.93%
Thymol:Menthol (1:1)	25.0%	1.37%	55.1%	3.06%

Decanoic acid:menthol (1:1) had consistent extraction rates and a narrow range for equilibrium of percent extracted. Decanoic acid:menthol (1:2) had two vials that were consistent and similar to decanoic acid:menthol (1:1), but one vial performed significantly worse. At the 5-h mark the sample increased 13% in percent of particles extracted indicating this vial had not reached its equilibrium yet. Thymol:menthol (1:1) had significantly worse extraction rates than the decanoic acid:menthol NADES. Percent of particles extracted fluctuated around the same values between 40 and 120 min but began to rise after 3 and 5 hours. In the timeframe of this experiment, none of the

thymol:menthol (1:1) vials reached equilibrium. The experiment was not extended like some of the polystyrene extractions due to the difference in OD readings not being as great as their corresponding concentration values.

3.3.5 Salt-water Extraction

Measurements taken during the extraction of plastic particles from salt-water proved to be inconsistent. The aggregation of the particles made it difficult to get an accurate representation of concentration by sampling only 40 μL or 200 μL . Taking larger samples and replacing after optical density readings might produce inaccurate results due to manual intervention and movement of particles from pipetting instead of stirring.

These challenges made it impossible to create a curve for rate of extraction, however, visual observations of extraction in salt-water suggest a significantly faster extraction. The aggregation of particles makes them more visible. For each plastic type, at the same concentrations as the freshwater experiments, most visible particles had transferred to the NADES phase after 10-20 min.

3.4 Statistical Analysis

Tables of the ANOVA and t-test results are included in APPENDIX 1.

3.4.1 Polymers across NADES

For PET, the initial rate of extraction for the three NADES were not significantly different (p-value = 0.46, Table 10) and the endpoints were not significantly different (p = 0.39, Table 19).

For PS, the initial rate of extraction for the three NADES were significantly different (p-value = 0.015, Table 11). There was a significant difference between the decanoic acid:menthol (1:1) and (1:2) extractions (p-value = 0.004, Table 12). There was no significant difference between the decanoic acid:menthol (1:1) and thymol:menthol (1:1) extractions (p-value = 0.43, Table 13) and between decanoic acid:menthol (1:2) and thymol:menthol (1:1) extractions (p-value = 0.069, Table 14). The endpoints for the three NADES were not significantly different (p-value = 0.33, Table 20).

For PLA, the ANOVA and pairwise t-tests were conducted excluding the outliers from decanoic acid:menthol (1:2). The initial rate of extraction for the three different solvents were significantly different (p-value=0.0096, Table 15). There was not a significant difference between the decanoic acid:menthol (1:1) and (1:2) extractions (p-value = 0.54, Table 16). There was a slightly significant difference between the acid:menthol (1:1) and thymol:menthol (1:1) extraction (p-value = 0.023, Table 17) and a slightly significant difference between the decanoic acid:menthol (1:2) and thymol:menthol (1:1) extraction (p-value = 0.040, Table 18).

The ANOVA for the PLA endpoint had a P-value of 0.013 indicating the three solvents were significantly different (Table 21). There was not a significant difference between the decanoic acid:menthol (1:1) and (1:2) endpoints (p-value = 0.54, Table 22). There was a slightly significant difference between the decanoic acid:menthol (1:1) and thymol:menthol (1:1) endpoint (p-value = 0.048, Table 23) and a significant difference between the decanoic acid acid:menthol (1:2) and thymol:menthol (1:1) endpoint (p-value = 0.0006, Table 24).

3.4.2 NADES across Polymers

For decanoic acid:menthol (1:1), the two-hour extraction for the three plastics were significantly different (p-value = 0.017, Table 25). There was no significant difference between the PET and PS extractions (p-value = 0.35, Table 26). There was a slightly significant difference between the PET and PLA extractions (p-value = 0.047, Table 27) and a significant difference between PS and PLA extractions (p-value = 0.013, Table 28). The endpoints for the three plastics were not significantly different (p-value = 0.20, Table 34).

For decanoic acid:menthol (1:2), the two-hour extraction for the three plastics were significantly different (p-value = 0.0004, Table 29). There was a significant difference between the PET and PS extractions (p-value = 0.0021, Table 30). There was a slightly significant difference between the PET and PLA extractions (p-value = 0.034, Table 31). There was a significant difference between PS and PLA extractions (p-value = 0.0016, Table 32). The endpoints for the three plastics were not significantly different (p-value = 0.17, Table 35).

For thymol:menthol (1:1), the two-hour extraction for the three NADES were not significantly different (p-value = 0.66, Table 33) and the endpoints were not significantly different (p = 0.10, Table 36).

3.5 Regression Model

Regression analysis of the extraction over time data was done using single rectangular curve fitting. This fitting is commonly used in enzyme kinetics as the Michaelis-Menten model where substrate concentration is plotted along the x-axis and

reaction rate is along the y-axis. The equation used to model the kinetics is

$v = V_{max} \frac{[S]}{K_M + [S]}$ where v is the rate of formation, V_{max} is the maximum rate achieved by the system, $[S]$ is the substrate concentration and K_M is the Michaelis-Menten constant that represents the substrate concentration where the reaction rate is half of the maximum rate. This model is also functionally identical to the Langmuir adsorption isotherm to describe adsorption on a particles surface.

This model was applied by Ilmi et al. (2017) to model the percent of production of fatty acid methyl esters in a liquid-liquid solid process over time (Ilmi, Kloekhorst et al. 2017). Using a similar reasoning, this model can be applied to the percent of plastic particles extracted over a period of time with the equation:

$$y = a \frac{x}{b + x}$$

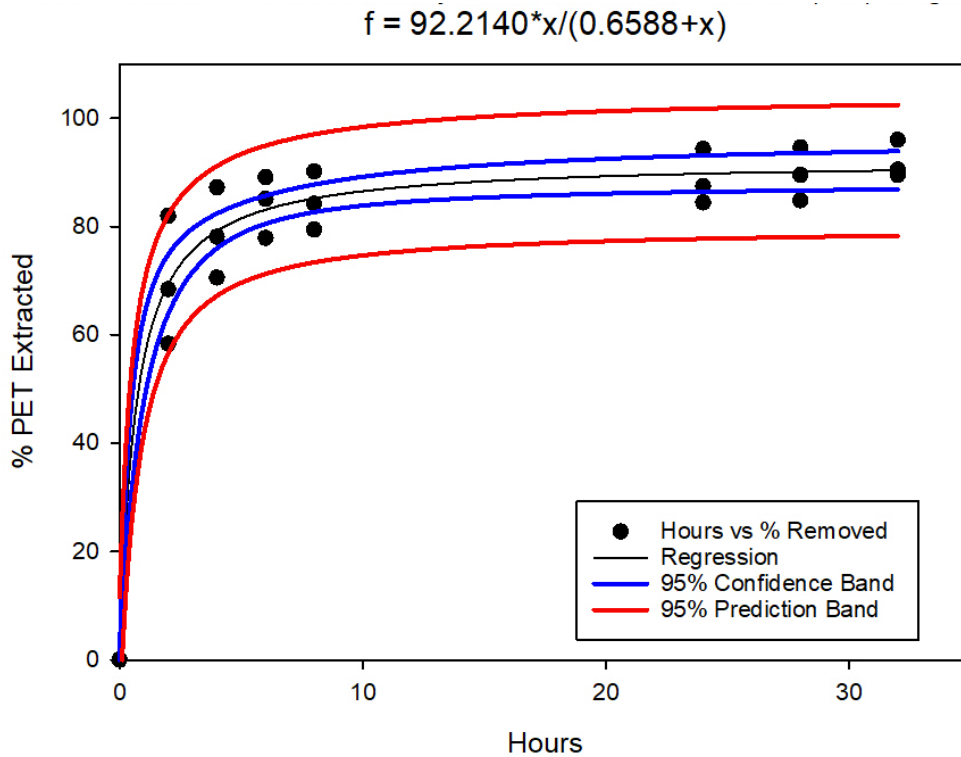
In this equation, y represents the percent of plastic particles extracted, x the time since the start of extraction, a the theoretical maximum of particles extracted from the aqueous phase, and b the time point where half of the theoretical maximum particles have been extracted from the aqueous phase.

Along with the regression, 95% confidence and 95% prediction bands were calculated. The 95% confidence interval shows the range at which we can be 95% confident a y -value will fall within given an x -value based on the statistical parameters of the system. The 95% prediction interval shows the range at which we can be 95% confident that a future observation will fall within given a certain x -value. Reports on the regression can be found in section 2 of APPENDIX 1.

3.5.1 PET

3.5.1.1 Decanoic Acid:Menthol (1:1)

The regression of the extraction of PET with decanoic acid:menthol (1:1) resulted in an R^2 value of 0.9662, an a value of 92.214 with a P-value < 0.0001 , and a b value of 0.6588 with a P-value < 0.0001 . The high R^2 value and low P-values for the coefficients suggest a statistically significant regression (Figure 14, Table 37).



3.5.1.2 Decanoic Acid:Menthol (1:2)

The regression of the extraction of PET with decanoic acid:menthol (1:2) resulted in an R^2 value of 0.9836, an a value of 93.1897 with a P-value < 0.0001 , and a b value of

0.6162 with a P-value < 0.0001. The high R^2 value and low P-values for the coefficients suggest a statistically significant regression (Figure 15, Table 38).

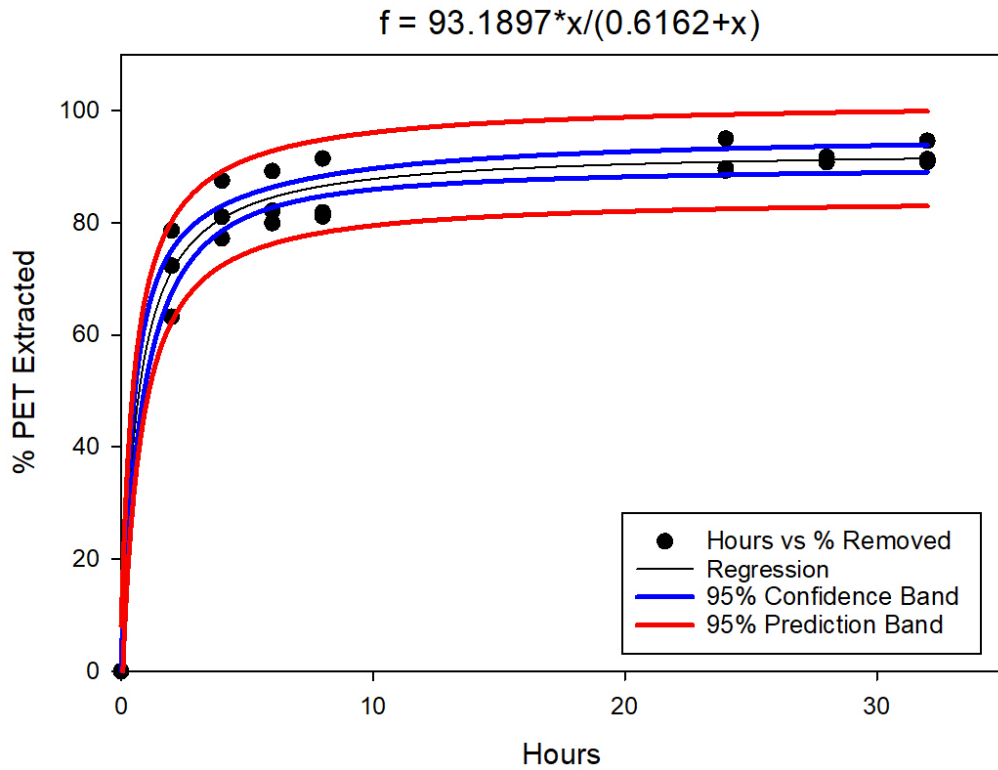


Figure 15 Percent of PET extracted by decanoic acid:menthol (1:2) regression

3.5.1.3 Thymol:Menthol (1:1)

The regression of the extraction of PET with thymol:menthol (1:1) resulted in an R^2 value of 0.9704, an a value of 90.7149 with a P-value < 0.0001, and a b value of 1.0183 with a P-value < 0.0001. The high R^2 value and low P-values for the coefficients suggest a statistically significant regression (Figure 16, Table 39).

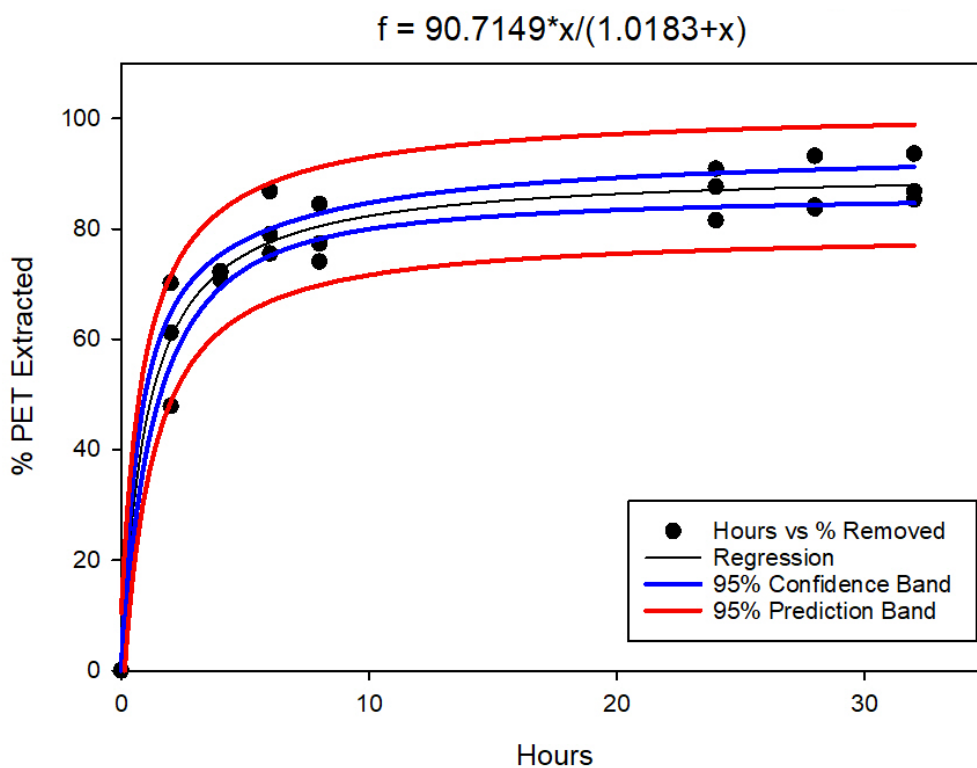


Figure 16 Percent of PET extracted by thymol:menthol (1:1) regression

3.5.1.4 Comparison of Regressions

As discussed previously, the coefficients from the regression show the theoretical maximum percentage of plastic particles extracted from the aqueous phase and the time point at which half of the maximum percentage of plastic particles have been extracted (Table 7). In general, the theoretical maximum determined by the regression are higher than the end-point experimental values. This can be explained by the theoretical maximum is the maximum point the reaction could reach if it continued for an indefinite amount of time. In the PET extraction regression, the two decanoic acid:menthol NADESs performed similarly and the thymol:menthol (1:1) NADES performing slightly worse. All three NADESs had theoretical maximums of at least 90% and extracted half of that maximum within or just past one hour of extraction.

Table 7 PET Regression Coefficient Comparison

	<i>a</i>	<i>b</i>
Decanoic Acid:Menthol (1:1)	92.21	0.66
Decanoic Acid:Menthol (1:2)	93.19	0.62
Thymol:Menthol (1:1)	90.71	1.02

A comparison of the regression lines from each of the three deep eutectic solvents in Figure 17.

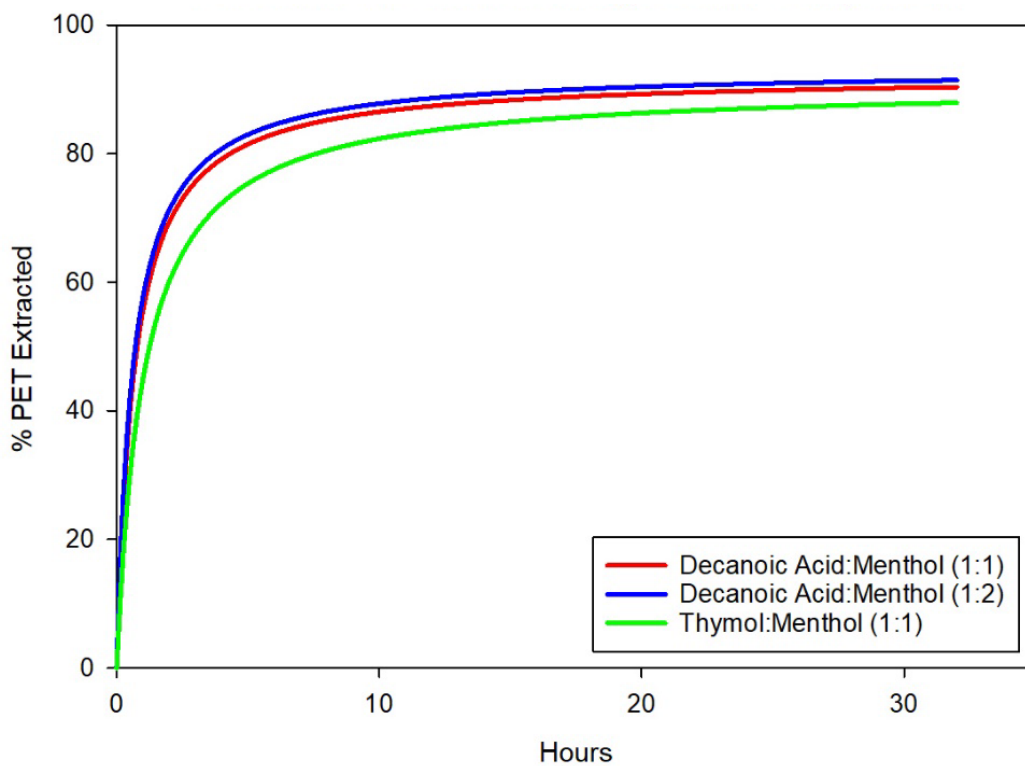


Figure 17 Percent of PET extracted regression comparison

3.5.2 PS

3.5.2.1 Decanoic Acid:Menthol (1:1)

The regression of the extraction of PS with decanoic acid:menthol (1:1) resulted in an R^2 value of 0.9541, an *a* value of 72.7804 with a P-value < 0.0001, and a *b* value of

0.9316 with a P-value < 0.0001. The high R^2 value and low P-values for the coefficients suggest a statistically significant regression (Figure 18, Table 40).

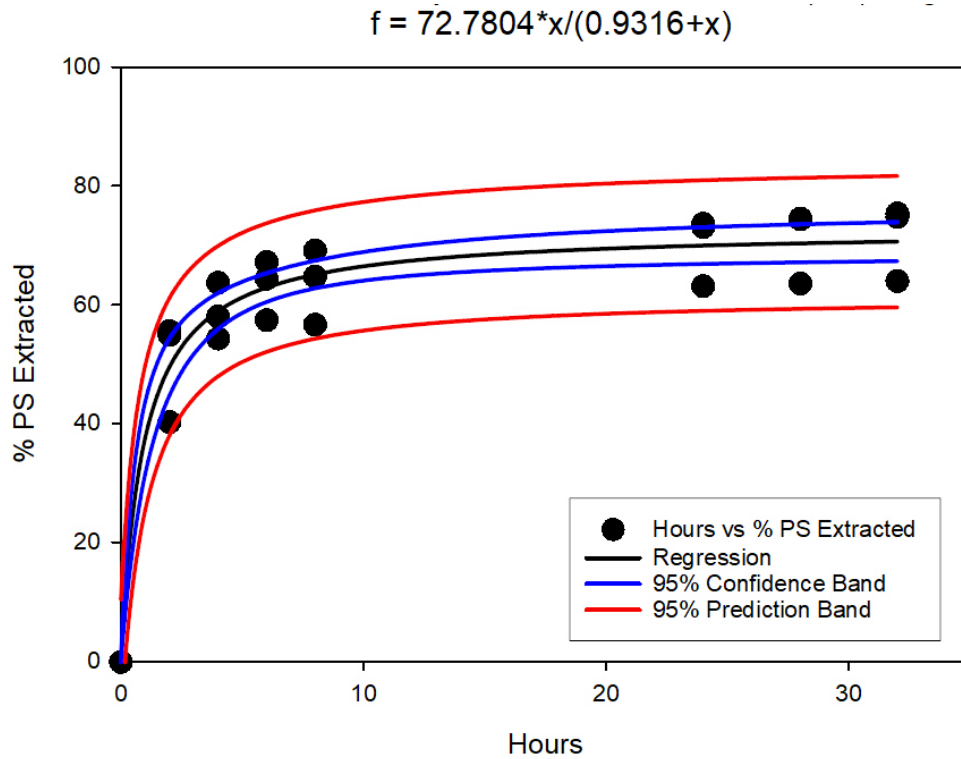


Figure 18 Percent of PS extracted by decanoic acid:menthol (1:1) regression

3.5.2.2 Decanoic Acid:Menthol (1:2)

The regression of the extraction of PS with decanoic acid:menthol (1:2) resulted in an R^2 value of 0.8632, an a value of 82.0796 with a P-value < 0.0001, and a b value of 16.7812 with a P-value of 0.0005. The high R^2 value and low P-values for the coefficients suggest a statistically significant regression (Figure 19, Table 41).

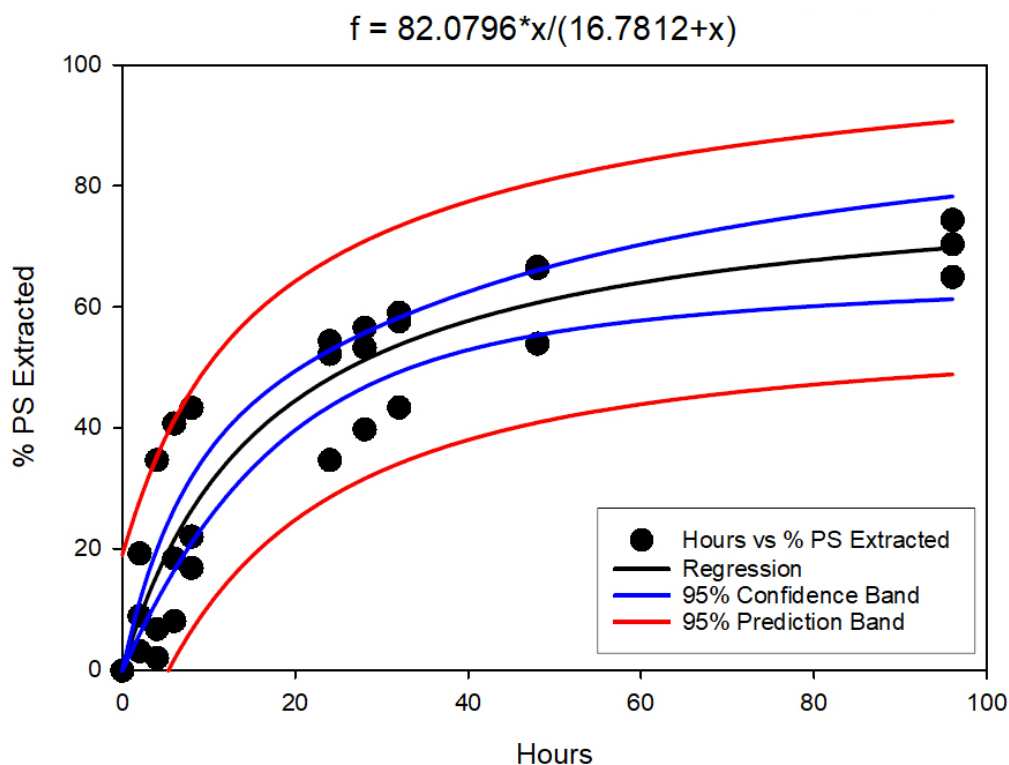


Figure 19 Percent of PS extracted by decanoic acid:menthol (1:2) regression

3.5.2.3 Thymol:Menthol (1:1)

The regression of the extraction of PS with thymol:menthol (1:1) resulted in an R^2 value of 0.7184, an a value of 62.5831 with a P-value < 0.0001 , and a b value of 1.1163 with a P-value of 0.0204. The lower R^2 value shows a worse fit than the other two regressions, but the low P-value for the a coefficient and the P-value of the b coefficient < 0.05 suggest a statistically significant regression (Figure 20, Table 42).

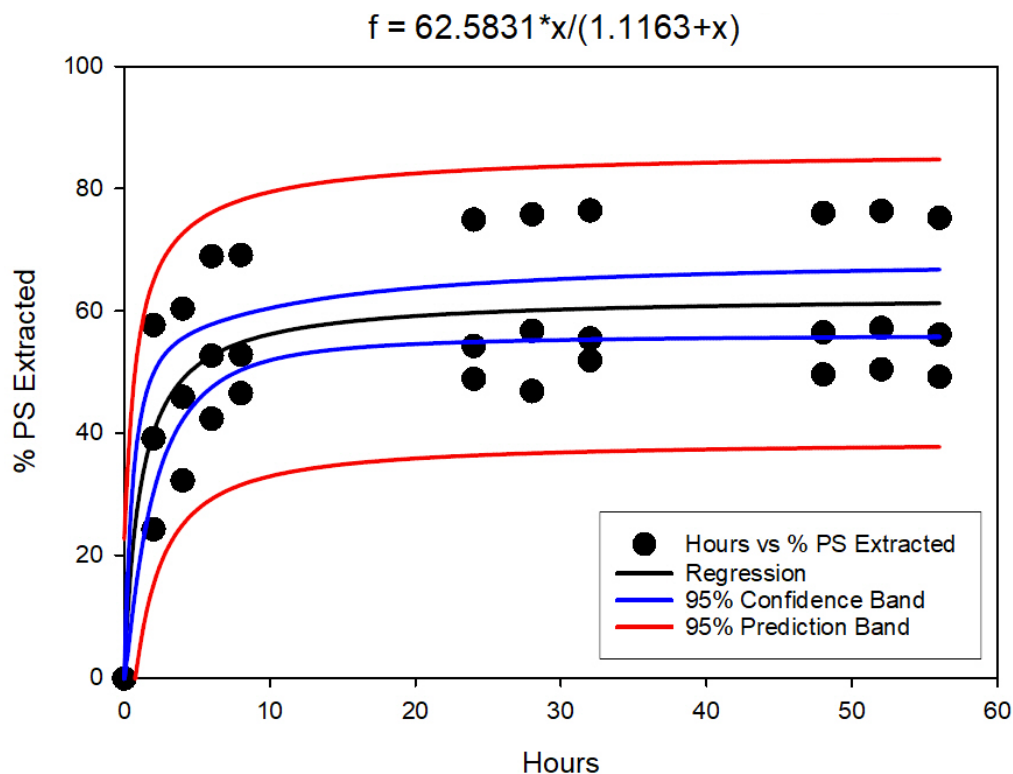


Figure 20 Percent of PS extracted by thymol:menthol (1:1) regression

3.5.2.4 Comparison of Regressions

In the PS extraction regression, the three NADESs had varying performances. According to the regression, decanoic acid:menthol (1:2) had the highest max of PS extracted at 82%, however, none of vials reached that level within the timeframe of this experiment. Decanoic acid:menthol (1:1) has a theoretical max of 72% and thymol:menthol (1:1) a max of 62%. Decanoic acid:menthol (1:1) and thymol:menthol (1:1) had similar extraction rates, reaching half of their max extraction after only one hour, while decanoic acid:menthol (1:2) had a significantly slower reaction rate taking almost 17 hours to reach half of its max extraction (Table 8).

Table 8 PS Regression Coefficient Comparison

	<i>a</i>	<i>b</i>
Decanoic Acid:Menthol (1:1)	72.78	0.93
Decanoic Acid:Menthol (1:2)	82.08	16.78
Thymol:Menthol (1:1)	62.58	1.12

A comparison of the regression lines from each of the three deep eutectic solvents in Figure 21.

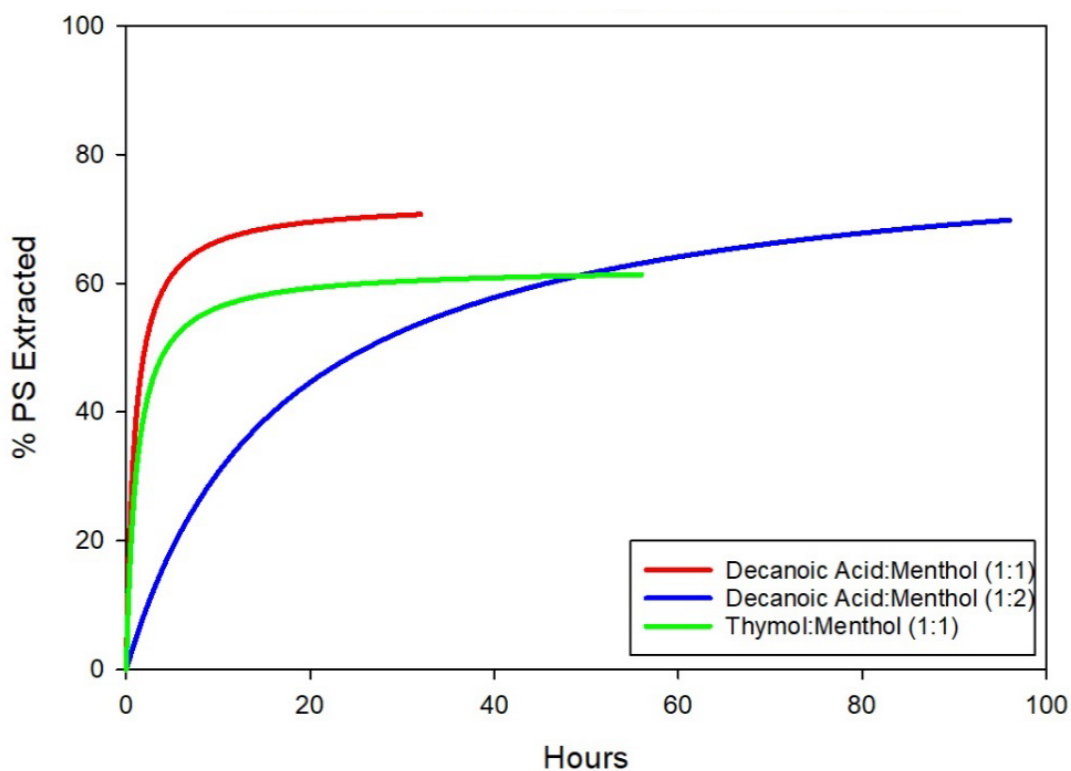


Figure 21 Percent of PS extracted regression comparison

3.5.3 PLA

3.5.3.1 Decanoic Acid:Menthol (1:1)

The regression of the extraction of PLA with decanoic acid:menthol (1:1) resulted in an R^2 value of 0.9250, an *a* value of 89.6455 with a P-value < 0.0001, and a *b* value of

13.5555 with a P-value of 0.0001. The high R^2 value and low P-values for the coefficients suggest a statistically significant regression (Figure 22, Table 43).

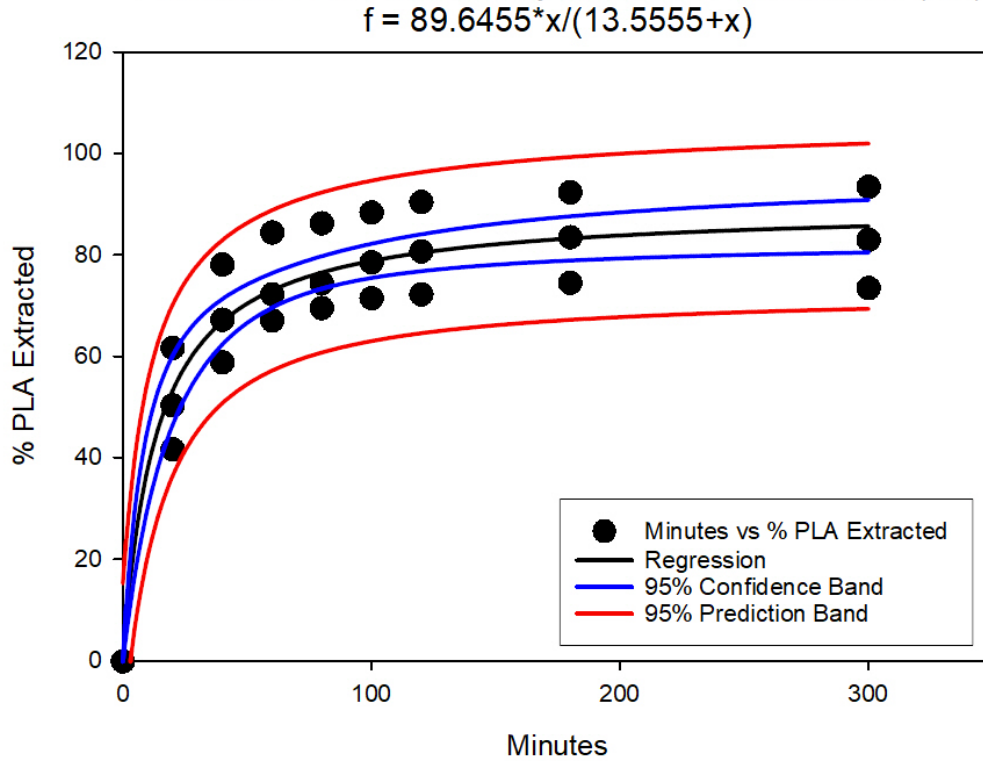


Figure 22 Percent of PLA extracted by decanoic acid:menthol (1:1) regression

3.5.3.2 Decanoic Acid:Menthol (1:2)

The regression of the extraction of PLA with decanoic acid:menthol (1:2) resulted in an R^2 value of 0.6131, an a value of 70.0071 with a P-value < 0.0001 , and a b value of 14.0254 with a P-value of 0.1133. The P-value for the a coefficient is low, but the low R^2 value and high P-value for the b coefficient suggests a poor fit and a statistically insignificant regression (Figure 23).

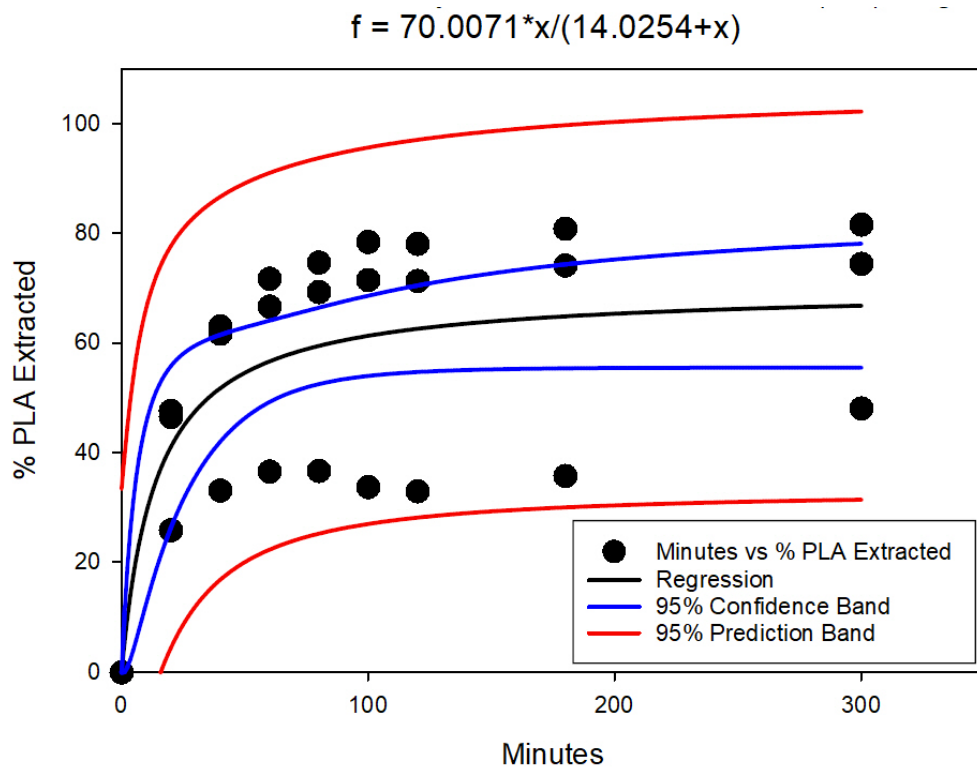


Figure 23 Percent of PLA extracted by decanoic acid:menthol (1:2) failed regression

If the data from the third vial are omitted as outliers, the regression of the extraction of PLA with decanoic acid:menthol (1:2) resulted in an R^2 value of 0.9852, an a value of 83.9470 with a P-value < 0.0001 , and a b value of 14.2660 with a P-value < 0.0001 . In this case the high R^2 value and low P-values for the coefficients suggest a statistically significant regression (Figure 24, Table 44).

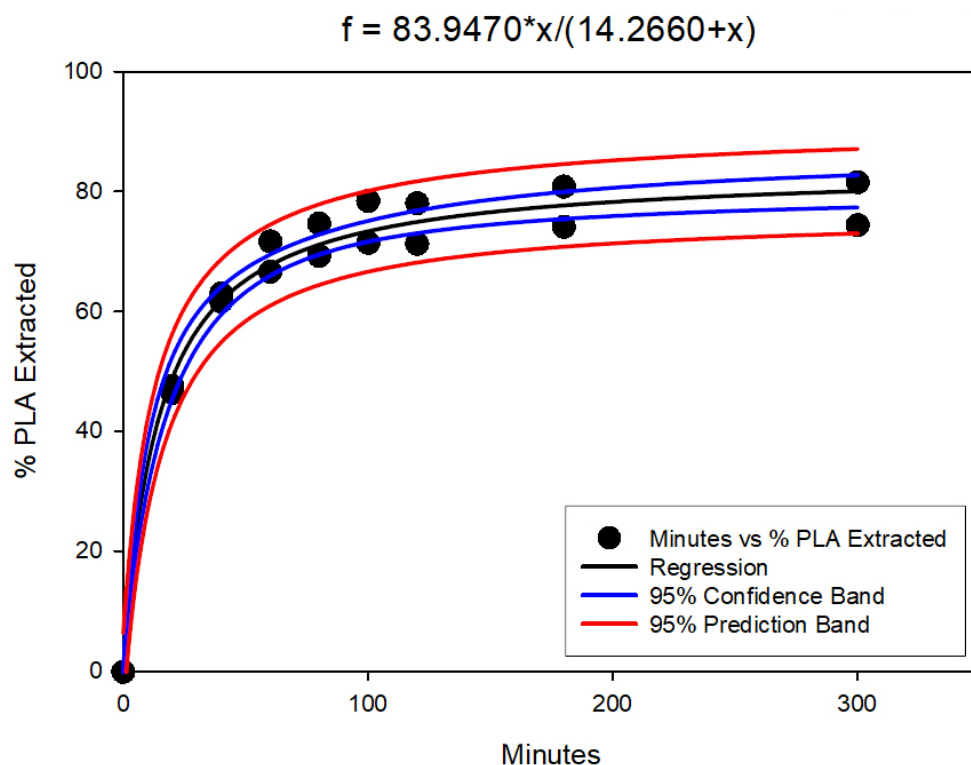


Figure 24 Percent of PLA extracted by decanoic acid:menthol (1:2) regression

3.5.3.3 Thymol:Menthol (1:1)

The regression of the extraction of PLA with thymol:menthol (1:1) resulted in an R^2 value of 0.8581, an a value of 49.4825 with a P-value < 0.0001, and a b value of 21.9126 with a P-value of 0.0011. The high R^2 value and low P-values for the coefficients suggest a statistically significant regression (Figure 25, Table 45). However, if the timeframe for this extraction had been extended, more plastic is likely to have been extracted due to the increase between the three- and five- hour marks. Therefore, this regression may be useful to predict where a sample may be within the timeframe of this experiment, but not to gauge what the maximum percentage of particles may be.

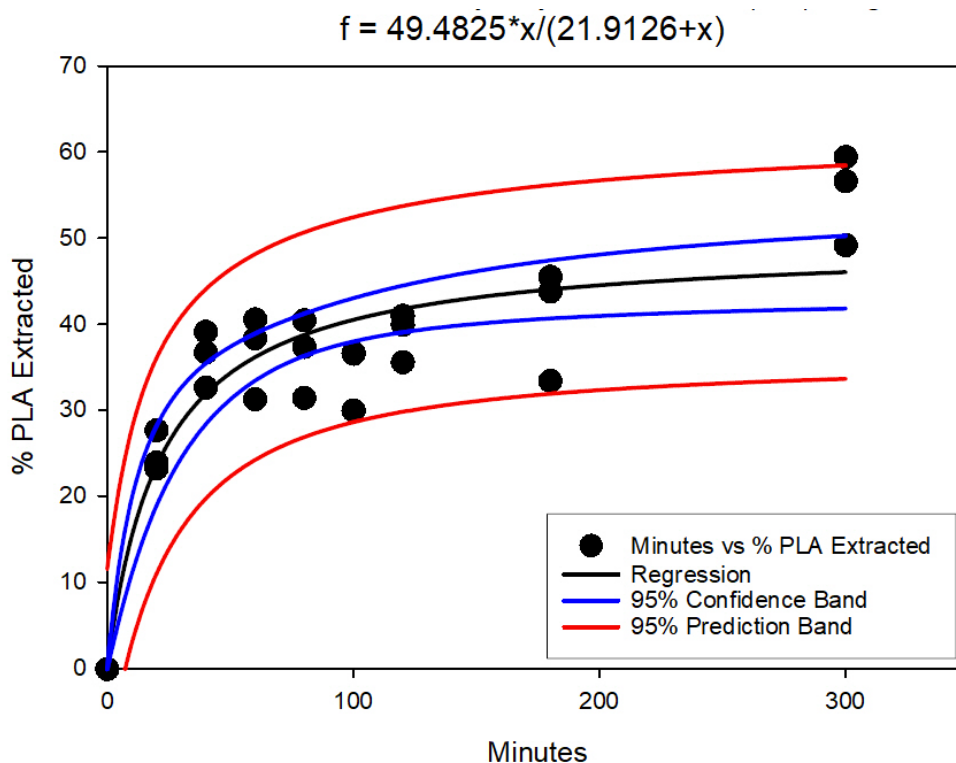


Figure 25 Percent of PLA extracted by thymol:menthol (1:1) regression

3.5.3.4 Comparison of Regressions

In the PLA extraction regression, the three NADESs had varying performances. The decanoic acid:menthol NADESs performed similarly with the (1:1) NADES having slightly higher maximum extraction and extraction rate than the (1:2). Thymol:menthol (1:1) had a much lower maximum extraction at less than 50% and a slower extraction rate, reaching half its maximum extraction 7 min slower than the other NADES (Table 9).

Table 9 PLA Regression Coefficient Comparison

	a	b (min)	b (h)
Decanoic Acid:Menthol (1:1)	89.65	13.56	0.226
Decanoic Acid:Menthol (1:2)	83.95	14.27	0.238
Thymol:Menthol (1:1)	49.48	21.91	0.365

A comparison of the regression lines from each of the three deep eutectic solvents in Figure 26.

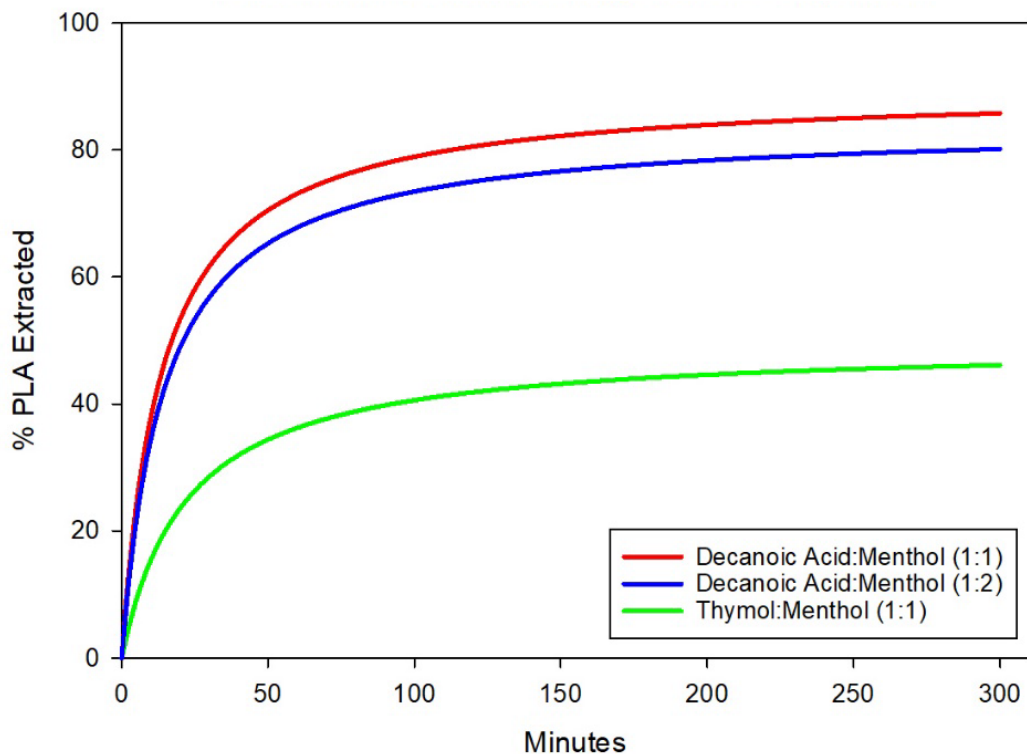


Figure 26 Percent of PLA extracted regression comparison

3.6 Simulation

Interactions between the plastic and NADES molecules within the simulation were measured by their radial distribution function (RDF), which describes the probability of finding a particle a given distance from a reference particle. A higher RDF indicates that the particle is more likely to associate with the reference particle. For PET and PLA, the chosen particles were the oxygen atoms, and the reference particles were the hydrogen atoms of hydroxyl groups on decanoic acid, menthol, and thymol. PS does not contain oxygen, so the four carbon atoms on the mainchain were used with the

hydrogens on the NADES. The RDF plots for decanoic acid:menthol (1:1) are shown in Figure 27, but the rest are included in APPENDIX 3.

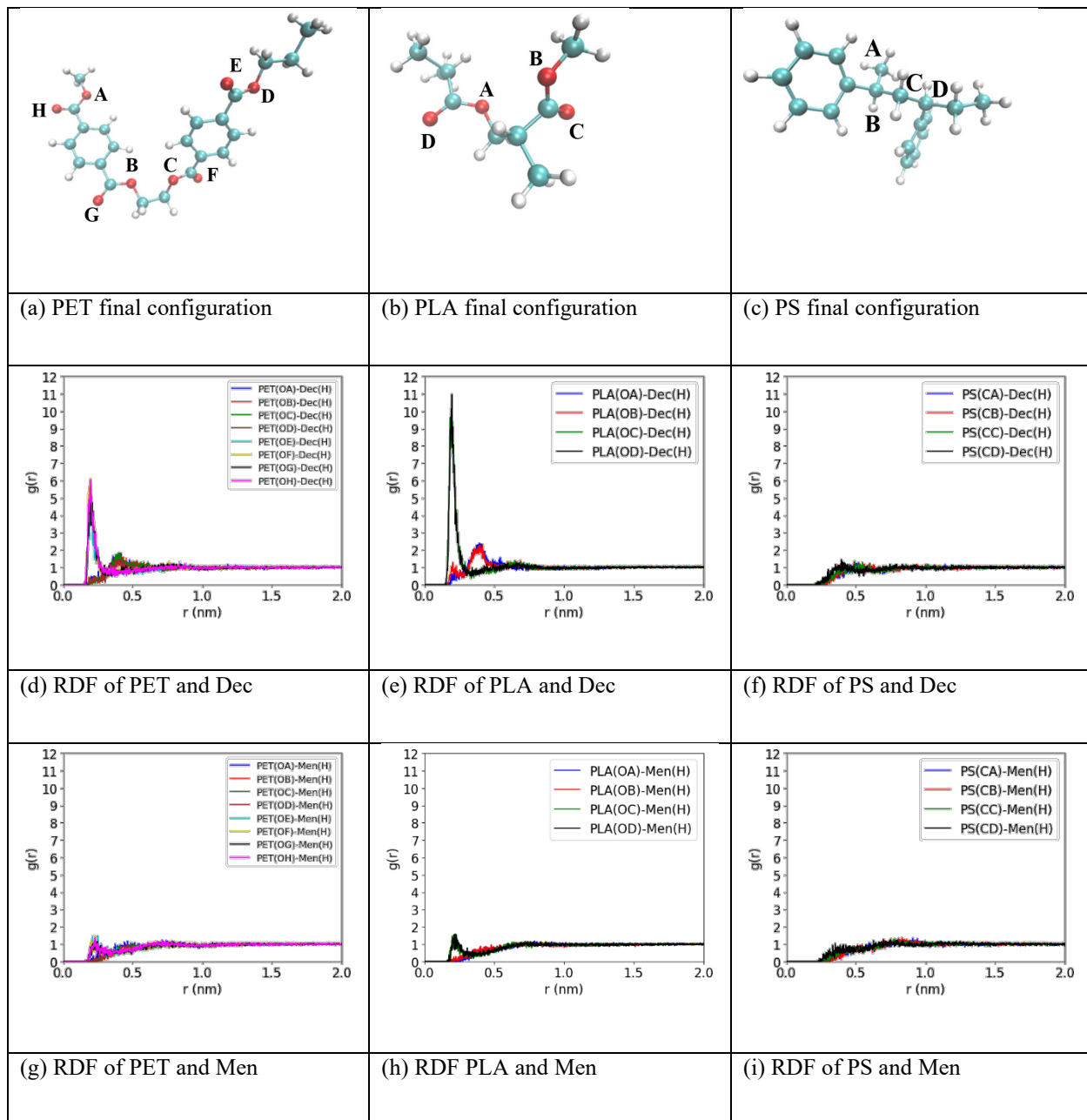


Figure 27 Final configuration and RDF results from the polymers in decanoic acid:menthol (1:1). (a)-(c) show the final configurations of PET, PLA, and PS in decanoic acid:menthol (1:1). (d) and (e) display the oxygen-hydrogen RDF between PET and PLA respectively with decanoic acid. (f) displays the carbon-hydrogen RDF between PS and decanoic acid. (g) and (h) display the oxygen-hydrogen RDF between PET and PLA respectively with menthol. (i) displays the carbon-hydrogen RDF between PS and menthol. The colors of the lines and legend represent the coordinating atom listed in Figure 28 in APPENDIX 3. (This figure was provided by Qi Qiao and represents results from her simulations.)

The final configuration for the polymers in decanoic acid:menthol (1:1) at 25 °C is shown in a-c. The RDF of each polymer with decanoic acid is shown in d-f and with menthol in g-i. The RDFs indicate that association between decanoic acid and PLA is the most likely, with PET as the second most likely, and PS having almost no association. The lack of any significant RDF peaks between the polymers and menthol also indicates that association between them is unlikely.

The results from decanoic acid:menthol (1:2) in Figure 30 are similar to decanoic acid:menthol (1:1), with no distinguishable difference in RDF for any of the polymers between the two NADES.

The results from thymol:menthol (1:1) in Figure 31 show smaller RDFs for PLA and PET with thymol than they did with decanoic acid, but still follow the trend of PLA having the largest, then PET, and almost no association with PS. The polymers had negligible RDF with menthol in this NADES as well.

The RDF of the polymers was determined with water for comparison, with the same atoms on the polymers and the hydrogen atoms of water as the reference. In Figure 32 it can be seen that each of the polymers showed no RDF peak, suggesting the polymers are unlikely to associate with water.

3.7 Discussion

The performance of NADES on extracting plastic particles can be organized by extraction rate and overall extraction efficiency. Overall, PLA was extracted at a higher or not significantly different rate of extraction and percent of particles extracted than the other polymers. PET was the second best at extraction, performing worse or not significantly different than PLA in some NADES and higher or not significantly different than PS, which performed the worst overall. Across the three tested NADESs, different plastic particle had different extraction rates, but no significant difference in overall percent of particles extracted.

For each of the polymers, decanoic acid:menthol (1:1) performed higher or not significantly different from the other NADES in both extraction rate and overall extraction. Decanoic acid:menthol (1:2) had similar performance with PET and PLA, but significantly slower extraction rate with PS. Thymol:menthol (1:1) had no significant difference in extraction performance to decanoic acid:menthol (1:1) with PET and PS, but worse in PLA.

The extraction of the plastic particles by hydrophobic NADES are influenced by several factors that contribute to the rate of extraction and the maximum percent of particles extracted. Some of the factors that were measured are the wettability of the polymers and NADES, the interactions between molecules of the polymers and NADES, and the size of the particles and the zeta potential.

3.7.1 Contact Angle and Wettability

The contact angle a liquid makes on a surface is a measurement of its wettability. Wetting measures the ability of a liquid to make and maintain contact with the surface of a solid and is influenced by intermolecular forces such as adhesion between the liquid and the solid and the cohesion within the liquid itself. Lower contact angles correlate to a higher wettability and extremely high wettability results in the spread of a liquid across the surface instead of forming a droplet.

The NADES mixtures showed much higher wettability on the commercially manufactured plastic films than water. On the PET film, there was no statistically significant difference between the initial angle for the two decanoic acid:menthol NADES mixtures, but for thymol:menthol (1:1) the initial angle was significantly higher. After contact, each of the NADES spread reaching angles lower than five, which is the minimum angle the instrument can measure, in all measurements but one thymol:menthol (1:1) and no significant difference was found. The PS film showed higher initial contact angles with no statistically significant difference between the NADES. After 30 seconds, the NADES spread with decanoic acid:menthol (1:1) being significantly higher and no significant difference between the other two NADES.

Between the two films, the decanoic acid:menthol (1:1) had an initial contact angle significantly higher on PS than PET, but there was no significant difference between the angles after 30 seconds. Decanoic acid:menthol (1:2) also had significantly different initial contact angles with PS being higher than PET, and by 30 seconds both had reached contact angles less than 5 degrees. Thymol:menthol (1:1) had no significant difference in initial contact angle or after 30 seconds.

For the polylactic acid film, there are variables hard to control during synthesis, such as surface roughness and thickness of the film. Due to this, the contact angle results are less consistent than the commercially manufactured PET and PS films. For instance, one of the decanoic acid:menthol (1:1) samples spread after initial contact and the other formed a droplet. Any comparisons between NADES would not be accurate representations of their interaction. However, the difference between the water and NADES are different to the point that the conclusion can be made that the NADES have more wettability on PLA than water.

3.7.2 Simulation

Results from the simulation systems show that there are interactions between the oxygen molecules on PLA and PET and the hydrogen molecules in decanoic acid and thymol. The RDFs between the polymers and NADES coordinate with the overall extraction data. The strongest association was between PLA and decanoic acid, which had the highest extraction rate as well as endpoint in decanoic acid:menthol (1:1) and performed well in decanoic acid:menthol (1:2). PLA in thymol:menthol (1:1) showed significantly lower initial extraction and at the endpoint. Considering PET was able to reach an extraction percent in thymol:menthol (1:1) that was not significantly different from the decanoic acid:menthol NADES, PLA may be able to reach a higher extraction if the timeframe was extended as is indicated by the increase at the five-hour mark.

PET had the second strongest association with the NADES and performed significantly lower than PLA at the two-hour extraction in both decanoic acid:menthol NADES, but not at the endpoints. In thymol:menthol (1:1), no significant difference was found between PET and PLA at the two-hour extraction point or at the endpoint.

PS showed no RDF with any of the NADES and performed worse or not significantly different than the other polymers in each of the NADES at both the two-hour point and the endpoint.

There was no significant difference in endpoint extractions across the polymers in each NADES which suggests that RDF is an indicator more on the extraction rate than the total percent of particles extracted.

3.7.3 Particle Size and Zeta Potential

The rate of extraction and maximum percentage of plastic extracted may be influenced by both the size of the particles and the zeta potential of the system. Nguyen et al. (2019) and Reimonn et al. (2019) have stated that one of greatest challenges in current separation techniques is particle size, with smaller particles reported to being more difficult to extract from an aqueous environment.

A well-recognized index for assessing the stability of a colloid system is zeta potential, with zeta potentials over $\pm 30\text{mV}$ being very stable, values between $\pm 15\text{-}30\text{mV}$ somewhat stable, and values between $\pm 0\text{-}15\text{mV}$ are prone to aggregate. The liquid layer surrounding a particle exists as an inner layer with strongly bonded ions and a diffuse layer further away where the particle is less firmly associated. Between these layers is a slipping plane and the potential across it is the zeta potential. The DVLO theory suggests that colloid stability is dependent on the total potential energy of a particle. The two majorly contributing forces are the van der Waals attractive and electric double layer repulsive forces. The equation to describe the van der Waals attractive force is $V_A = \frac{-A}{12 \Pi D^2}$ where A is the Hamaker constant, Π is the solvent permeability, and D is the

particle separation. The equation for the electric double layer repulsive forces is $V_R = 2\Pi a \zeta^2 e^{-\kappa D}$ where a is the particle radius, ζ is the zeta potential, and κ is a function of the ionic composition. If the repulsive forces are greater than the attractive forces, the particles will stay separated and form a colloidal system. From the equation for repulsive forces, both particle size and zeta potential have an influence on the stability of suspension of particles. However, if the particles are too large, the inertial and gravitational forces will have a larger impact than the attractive and repulsive forces and prevent a colloid from forming. In the extraction experiment each particle had the same initial concentration, but the stocks with a larger particle size would have a greater particle separation, which will also have a significant influence over both the repulsive and attractive forces.

Applying these equations to the results from the dynamic light scattering can partially explain why the particles had different rates of extractions from DI water. The particles were extracted at a rate from highest to lowest in the order of largest to smallest particle size and smallest to largest zeta potential. The average size of the PLA particles were two to three times the size of the PET and PS particles, which would increase the separation of the particles dramatically and have more influence from gravitational forces, which would explain the much faster rate of extraction. Between the PET and PS particles, the PET had a larger particle size and lower zeta potential and was extracted at a faster rate, but this can only partially explain difference as the PS extraction rates were significantly different across the three NADES. No significant difference in maximum percent of particles extracted were found across for each NADES in extracting the

different polymers, suggesting that the size of the particles does not play a significant role in the maximum percentage of particles extracted.

In salt-water, the size of the measured particles increased due to aggregation, and the zeta potential became less negative. As the zeta potential decreases, the repulsive forces decrease and once the attractive forces are larger, the suspension becomes unstable, and particles will aggregate. It has been documented in previous studies that the addition of sodium chloride to a solution will decrease the negativity of zeta potential around particles. Prathapan et al. (2016) reported a less negative zeta potential of cellulosic nanocrystals in increasing concentrations of sodium chloride (Prathapan, Thapa et al. 2016). The introduction of sodium ions encourages adsorption to the surface of the particles and compresses the size of the double layer. In some cases, the adsorption of ions can even reverse the charge on the surface, which was observed in the case of PLA in the sodium chloride solution.

CHAPTER 4. CONCLUSIONS AND FUTURE WORK

4.1 Conclusions

The aim of this project was to investigate the ability of the chosen hydrophobic natural NADES solvents to extract nano-particles of synthetic polymers in a liquid-liquid extraction system. Three objectives were set for this investigation.

The first objective was to synthesize and characterize the NADES to have a better understanding of their affinity toward the polymers in comparison to water. To achieve this, the contact angles of a droplet of each NADES and water were measured on a film of each polymer. The contact angle given measures its wettability or its ability to make

and maintain contact with a surface. The contact angles of the NADES on each film were significantly less than the contact angle of water, suggesting the NADES are more likely to adhere to the surface of the polymers than water is and potentially making extraction from the water phase more likely.

The higher affinity between NADES and polymer is further backed up from simulation data. The RDF calculated between oxygen atoms in PET and PLA with the hydrogens in decanoic acid and thymol suggest there are significant interactions between the molecules, while the RDF with water suggested no significant interactions.

The second objective was to develop a method to synthesize nano-particles of each polymer and characterize the particles. A method for synthesizing the nano-particles was achieved, however, controlling the size of the particles proved to be difficult. Particle size, zeta potential, and distance between particles all influence the stability of a suspension of particles within an aqueous environment. Larger particles with more distance between particles and a zeta potential closer to zero have a less stable suspensions making them more likely to move to more favorable environment. The particle size and zeta potential were measured, with PLA having the largest average diameter, followed by PET, and then PS. The zeta potentials of these polymers were negatively charged with the most negative being PS, followed by PET, and PLA.

The extraction experiments show that each of the NADES was able to successfully extract each of the polymers to a significant degree. The polymer extracted at the highest rate was PLA, followed by PET, and then PS. Overall, each of the NADES had no significant difference in the maximum percentage of polymer particles extracted. For each polymer, decanoic acid:menthol (1:1) was the most consistent with the highest

or equal extraction rates to the others. Decanoic acid:menthol (1:2) extracting PET and PLA at a similar rate but was significantly slower extracting PS. Thymol:menthol (1:1) had no significant difference in extraction rate from decanoic acid:menthol (1:1) in PET and PS but was significantly slower in extracting PLA. The maximum percent of PET and PS particles extracted were not significantly different across the three NADES, but PLA had a significantly lower maximum than with thymol:menthol (1:1) than the other NADES. This could be due to the shorter timeframe used in the PLA extraction and if extended, it could reach a similar level.

These results coordinate with the characterization work done with the NADES and polymers. PLA, the polymer with the highest affinity to the NADES, the largest particle size, and least stable suspension was extracted at the highest rate. PS was the polymer with the least affinity to the NADES, the smallest particle size, and the most stable suspension was extracted at the slowest rate.

4.2 Future Work

Due to time constraints, there is more work that can be done on this subject in the future. Refining the method to synthesize the nano-particles of the polymers to have a more uniform particle size would help control a potentially significant variable within this study. It is difficult to measure how much of an impact the size of the polymers has on the extraction rates compared to the differences in NADES.

Some of the experiments should be repeated with extended timeframes. In the extraction of PLA with thymol:menthol (1:1), the experiment was stopped at the same

point as the other PLA extractions, but the last measurements suggest that the extraction had not yet reached equilibrium.

More characterization work can be done on the NADES such as FTIR and melting point analysis. Particle size and zeta potential could be conducted on water phase post extraction to determine if certain sized particles are extracted first and if the zeta potential changes over the course of the extraction.

Studies of biocompatibility of DES and NADES have shown favorable results and in recent years there have been enzymes discovered that have the capability to depolymerize certain types of synthetic polymers. It may be worth exploring a system using DES or NADES within an enzymatic depolymerization system.

APPENDICES

1. APPENDIX 1: STATISTICAL ANALYSIS TABLES

1.1. Polymer Extraction Tables

Table 10 PET Initial Extraction ANOVA

Anova: Single Factor						
SUMMARY						
<i>Groups</i>	<i>Count</i>	<i>Sum</i>	<i>Average</i>	<i>Variance</i>		
Decanoic acid:menthol (1:1)	3	1.759045	0.586348	0.010813		
Decanoic acid:menthol (1:2)	3	1.64641	0.548803	0.005096		
Thymol:menthol (1:1)	3	1.430752	0.476917	0.015249		
ANOVA						
<i>Source of Variation</i>	<i>SS</i>	<i>df</i>	<i>MS</i>	<i>F</i>	<i>P-value</i>	<i>F crit</i>
Between Groups	0.018552	2	0.009276	0.893126	0.457581	5.143253
Within Groups	0.062317	6	0.010386			
Total	0.08087	8				

Table 11 PS Initial Extraction ANOVA

Anova: Single Factor						
SUMMARY						
<i>Groups</i>	<i>Count</i>	<i>Sum</i>	<i>Average</i>	<i>Variance</i>		
Decanoic acid:menthol (1:1)	3	1.509956	0.503319	0.007519		
Decanoic acid:menthol (1:2)	3	0.315298	0.105099	0.006689		
Thymol:menthol (1:1)	3	1.213645	0.404548	0.028055		
ANOVA						
<i>Source of Variation</i>	<i>SS</i>	<i>df</i>	<i>MS</i>	<i>F</i>	<i>P-value</i>	<i>F crit</i>
Between Groups	0.258004	2	0.129002	9.156959	0.015028	5.143253
Within Groups	0.084527	6	0.014088			
Total	0.342531	8				

Table 12 PS Initial Extraction t-test DA:M(1:1) & DA:M(1:2)

t-Test: Two-Sample Assuming Unequal Variances		
	<i>DA:M(1:1)</i>	<i>DA:M(1:2)</i>
Mean	0.503318534	0.105099407
Variance	0.007519003	0.006689481
Observations	3	3
Hypothesized Mean Difference	0	
df	4	
t Stat	5.786405526	
P(T<=t) one-tail	0.002216197	
t Critical one-tail	2.131846786	
P(T<=t) two-tail	0.004432394	
t Critical two-tail	2.776445105	

Table 13 PS Initial Extraction t-test DA:M(1:1) & T:M(1:1)

t-Test: Two-Sample Assuming Unequal Variances		
	<i>DA:M(1:1)</i>	<i>T:M(1:1)</i>
Mean	0.503318534	0.404548421
Variance	0.007519003	0.028055063
Observations	3	3
Hypothesized Mean Difference	0	
df	3	
t Stat	0.907025348	
P(T<=t) one-tail	0.215629868	
t Critical one-tail	2.353363435	
P(T<=t) two-tail	0.431259737	
t Critical two-tail	3.182446305	

Table 14 PS Initial Extraction t-test DA:M(1:2) & T:M(1:1)

t-Test: Two-Sample Assuming Unequal Variances		
	<i>DA:M(1:2)</i>	<i>T:M(1:1)</i>
	<i>Variable 1</i>	<i>Variable 2</i>
Mean	0.105099407	0.404548421
Variance	0.006689481	0.028055063
Observations	3	3
Hypothesized Mean Difference	0	
df	3	
t Stat	2.782532237	
P(T<=t) one-tail	0.034422665	
t Critical one-tail	2.353363435	
P(T<=t) two-tail	0.068845329	
t Critical two-tail	3.182446305	

Table 15 PLA Initial Extraction ANOVA

Anova: Single Factor						
Initial Rate						
SUMMARY						
<i>Groups</i>	<i>Count</i>	<i>Sum</i>	<i>Average</i>	<i>Variance</i>		
Decanoic acid:menthol (1:1)	3	1.539335	0.513112	0.010107		
Decanoic acid:menthol (1:2)	2	0.941903	0.470951	6.08E-05		
Thymol:menthol (1:1)	3	0.75	0.25	0.000564		
ANOVA						
<i>Source of Variation</i>	<i>SS</i>	<i>df</i>	<i>MS</i>	<i>F</i>	<i>P-value</i>	<i>F crit</i>
Between Groups	0.115829	2	0.057914	13.52925	0.009607	5.786135
Within Groups	0.021403	5	0.004281			
Total	0.137232	7				

Table 16 PLA Initial Extraction t-test DA:M(1:1) & DA:M(1:2)

t-Test: Two-Sample Assuming Unequal Variances		
	<i>DA:M(1:1)</i>	<i>DA:M(1:2)</i>
Mean	0.83388194	0.780612245
Variance	0.009937336	0.002574586
Observations	3	2
Hypothesized Mean Difference	0	
df	3	
t Stat	0.785441139	
P(T<=t) one-tail	0.244757595	
t Critical one-tail	2.353363435	
P(T<=t) two-tail	0.48951519	
t Critical two-tail	3.182446305	

Table 17 PLA Initial Extraction t-test DA:M(1:1) & T:M(1:1)

t-Test: Two-Sample Assuming Unequal Variances		
	<i>DA:M(1:1)</i>	<i>T:M(1:1)</i>
Mean	0.83388194	0.551239851
Variance	0.009937336	0.00280657
Observations	3	3
Hypothesized Mean Difference	0	
df	3	
t Stat	4.336568215	
P(T<=t) one-tail	0.011311986	
t Critical one-tail	2.353363435	
P(T<=t) two-tail	0.022623972	
t Critical two-tail	3.182446305	

Table 18 PLA Initial Extraction t-test DA:M(1:2) & T:M(1:1)

t-Test: Two-Sample Assuming Unequal Variances		
	<i>DA:M(1:2)</i>	<i>T:M(1:1)</i>
Mean	0.780612245	0.551239851
Variance	0.002574586	0.00280657
Observations	2	3
Hypothesized Mean Difference	0	
df	2	
t Stat	4.865072698	
P(T<=t) one-tail	0.019873767	
t Critical one-tail	2.91998558	
P(T<=t) two-tail	0.039747533	
t Critical two-tail	4.30265273	

Table 19 PET Endpoint Extraction ANOVA

Anova: Single Factor						
SUMMARY						
<i>Groups</i>	<i>Count</i>	<i>Sum</i>	<i>Average</i>	<i>Variance</i>		
Decanoic acid:menthol (1:1)	3	2.32377	0.77459	0.001227		
Decanoic acid:menthol (1:2)	3	2.124081	0.708027	0.00074		
Thymol:menthol (1:1)	3	2.250424	0.750141	0.007186		
ANOVA						
<i>Source of Variation</i>	<i>SS</i>	<i>df</i>	<i>MS</i>	<i>F</i>	<i>P-value</i>	<i>F crit</i>
Between Groups	0.006802	2	0.003401	1.11483	0.387532	5.143253
Within Groups	0.018304	6	0.003051			
Total	0.025106	8				

Table 20 PS Endpoint Extraction ANOVA

Anova: Single Factor						
SUMMARY						
<i>Groups</i>	<i>Count</i>	<i>Sum</i>	<i>Average</i>	<i>Variance</i>		
Decanoic acid:menthol (1:1)	3	2.143539	0.714513	0.004098		
Decanoic acid:menthol (1:2)	3	2.099853	0.699951	0.002233		
Thymol:menthol (1:1)	3	1.808397	0.602799	0.018121		
ANOVA						
<i>Source of Variation</i>	<i>SS</i>	<i>df</i>	<i>MS</i>	<i>F</i>	<i>P-value</i>	<i>F crit</i>
Between Groups	0.022131	2	0.011065	1.357591	0.326305	5.143253
Within Groups	0.048904	6	0.008151			
Total	0.071035	8				

Table 21 PLA Endpoint Extraction ANOVA

Anova: Single Factor						
Endpoint						
SUMMARY						
<i>Groups</i>	<i>Count</i>	<i>Sum</i>	<i>Average</i>	<i>Variance</i>		
Decanoic acid:menthol (1:1)	3	2.501646	0.833882	0.009937		
Decanoic acid:menthol (1:2)	2	1.561224	0.780612	0.002575		
Thymol:menthol (1:1)	3	1.65372	0.55124	0.002807		
ANOVA						
<i>Source of Variation</i>	<i>SS</i>	<i>df</i>	<i>MS</i>	<i>F</i>	<i>P-value</i>	<i>F crit</i>
Between Groups	0.131459	2	0.06573	11.71135	0.01298	5.786135
Within Groups	0.028062	5	0.005612			
Total	0.159522	7				

Table 22 PLA Endpoint Extraction t-test DA:M(1:1) & DA:M(1:2)

t-Test: Two-Sample Assuming Unequal Variances		
	<i>DA:M(1:1)</i>	<i>DA:M(1:2)</i>
Mean	0.513111696	0.470951284
Variance	0.010106848	6.07973E-05
Observations	3	2
Hypothesized Mean Difference	0	
df	2	
t Stat	0.723114467	
P(T<=t) one-tail	0.272371044	
t Critical one-tail	2.91998558	
P(T<=t) two-tail	0.544742087	
t Critical two-tail	4.30265273	

Table 23 PLA Endpoint Extraction t-test DA:M(1:1) & T:M(1:1)

t-Test: Two-Sample Assuming Unequal Variances		
	<i>DA:M(1:1)</i>	<i>T:M(1:1)</i>
Mean	0.513111696	0.25
Variance	0.010106848	0.000564471
Observations	3	3
Hypothesized Mean Difference	0	
df	2	
t Stat	4.411555505	
P(T<=t) one-tail	0.023866808	
t Critical one-tail	2.91998558	
P(T<=t) two-tail	0.047733616	
t Critical two-tail	4.30265273	

Table 24 PLA Endpoint Extraction t-test DA:M(1:2) & T:M(1:1)

t-Test: Two-Sample Assuming Unequal Variances		
	<i>DA:M(1:2)</i>	<i>T:M(1:1)</i>
Mean	0.470951284	0.25
Variance	6.07973E-05	0.000564471
Observations	2	3
Hypothesized Mean Difference	0	
df	3	
t Stat	14.94567899	
P(T<=t) one-tail	0.000325041	
t Critical one-tail	2.353363435	
P(T<=t) two-tail	0.000650082	
t Critical two-tail	3.182446305	

Table 25 Decanoic Acid:Menthol (1:1) Two Hour Extraction ANOVA

Anova: Single Factor						
SUMMARY						
<i>Groups</i>	<i>Count</i>	<i>Sum</i>	<i>Average</i>	<i>Variance</i>		
PET	3	1.759045	0.586348	0.010813		
PS	3	1.509956	0.503319	0.007519		
PLA	3	2.436142	0.812047	0.008251		
ANOVA						
<i>Source of Variation</i>	<i>SS</i>	<i>df</i>	<i>MS</i>	<i>F</i>	<i>P-value</i>	<i>F crit</i>
Between Groups	0.153148	2	0.076574	8.641394	0.017114	5.143253
Within Groups	0.053168	6	0.008861			
Total	0.206315	8				

Table 26 Decanoic Acid:Menthol (1:1) Initial Extraction t-test PET & PS

t-Test: Two-Sample Assuming Unequal Variances		
	<i>PET</i>	<i>PS</i>
Mean	0.586348	0.503319
Variance	0.010813	0.007519
Observations	3	3
Hypothesized Mean Difference	0	
df	4	
t Stat	1.062144	
P(T<=t) one-tail	0.174021	
t Critical one-tail	2.131847	
P(T<=t) two-tail	0.348043	
t Critical two-tail	2.776445	

Table 27 Decanoic Acid:Menthol (1:1) Initial Extraction t-test PET & PLA

t-Test: Two-Sample Assuming Unequal Variances		
	<i>PET</i>	<i>PLA</i>
Mean	0.586348	0.812047
Variance	0.010813	0.008251
Observations	3	3
Hypothesized Mean Difference	0	
df	4	
t Stat	-2.83122	
P(T<=t) one-tail	0.023643	
t Critical one-tail	2.131847	
P(T<=t) two-tail	0.047286	
t Critical two-tail	2.776445	

Table 28 Decanoic Acid:Menthol (1:1) Initial Extraction t-test PS & PLA

t-Test: Two-Sample Assuming Unequal Variances		
	<i>PS</i>	<i>PLA</i>
Mean	0.503319	0.812047
Variance	0.007519	0.008251
Observations	3	3
Hypothesized Mean Difference	0	
df	4	
t Stat	-4.25811	
P(T<=t) one-tail	0.006537	
t Critical one-tail	2.131847	
P(T<=t) two-tail	0.013073	
t Critical two-tail	2.776445	

Table 29 Decanoic Acid:Menthol (1:2) Two Hour Extraction ANOVA

Anova: Single Factor						
SUMMARY						
<i>Groups</i>	<i>Count</i>	<i>Sum</i>	<i>Average</i>	<i>Variance</i>		
PET	3	1.64641	0.548803	0.005096		
PS	3	0.315298	0.105099	0.006689		
PLA	2	1.495063	0.747531	0.002299		
ANOVA						
<i>Source of Variation</i>	<i>SS</i>	<i>df</i>	<i>MS</i>	<i>F</i>	<i>P-value</i>	<i>F crit</i>
Between Groups	0.560641	2	0.280321	54.17772	0.000409	5.786135
Within Groups	0.02587	5	0.005174			
Total	0.586511	7				

Table 30 Decanoic Acid:Menthol (1:2) Initial Extraction t-test PET & PS

t-Test: Two-Sample Assuming Unequal Variances		
	<i>PET</i>	<i>PS</i>
Mean	0.548803	0.105099
Variance	0.005096	0.006689
Observations	3	3
Hypothesized Mean Difference	0	
df	4	
t Stat	7.079055	
P(T<=t) one-tail	0.001051	
t Critical one-tail	2.131847	
P(T<=t) two-tail	0.002102	
t Critical two-tail	2.776445	

Table 31 Decanoic Acid:Menthol (1:2) Initial Extraction t-test PET & PLA

t-Test: Two-Sample Assuming Unequal Variances		
	<i>PET</i>	<i>PLA</i>
Mean	0.548803	0.747531
Variance	0.005096	0.002299
Observations	3	2
Hypothesized Mean Difference	0	
df	3	
t Stat	-3.72367	
P(T<=t) one-tail	0.016861	
t Critical one-tail	2.353363	
P(T<=t) two-tail	0.033722	
t Critical two-tail	3.182446	

Table 32 Decanoic Acid:Menthol (1:2) Initial Extraction t-test PS & PLA

t-Test: Two-Sample Assuming Unequal Variances		
	<i>PS</i>	<i>PLA</i>
Mean	0.105099	0.747531
Variance	0.006689	0.002299
Observations	3	2
Hypothesized Mean Difference	0	
df	3	
t Stat	-11.0513	
P(T<=t) one-tail	0.000793	
t Critical one-tail	2.353363	
P(T<=t) two-tail	0.001587	
t Critical two-tail	3.182446	

Table 33 Thymol:Menthol (1:1) Two Hour Extraction ANOVA

Anova: Single Factor						
SUMMARY						
<i>Groups</i>	<i>Count</i>	<i>Sum</i>	<i>Average</i>	<i>Variance</i>		
PET	3	1.430752	0.476917	0.015249		
PS	3	1.213645	0.404548	0.028055		
PLA	3	1.166722	0.388907	0.000808		
ANOVA						
<i>Source of Variation</i>	<i>SS</i>	<i>df</i>	<i>MS</i>	<i>F</i>	<i>P-value</i>	<i>F crit</i>
Between Groups	0.013228	2	0.006614	0.449798	0.657632	5.143253
Within Groups	0.088224	6	0.014704			
Total	0.101452	8				

Table 34 Decanoic Acid:Menthol (1:1) Endpoint Extraction ANOVA

Anova: Single Factor						
SUMMARY						
<i>Groups</i>	<i>Count</i>	<i>Sum</i>	<i>Average</i>	<i>Variance</i>		
PET	3	2.32377	0.77459	0.001227		
PS	3	2.143539	0.714513	0.004098		
PLA	3	2.501646	0.833882	0.009937		
ANOVA						
<i>Source of Variation</i>	<i>SS</i>	<i>df</i>	<i>MS</i>	<i>F</i>	<i>P-value</i>	<i>F crit</i>
Between Groups	0.021374	2	0.010687	2.100664	0.203462	5.143253
Within Groups	0.030524	6	0.005087			
Total	0.051898	8				

Table 35 Decanoic Acid:Menthol (1:2) Endpoint Extraction ANOVA

Anova: Single Factor						
SUMMARY						
<i>Groups</i>	<i>Count</i>	<i>Sum</i>	<i>Average</i>	<i>Variance</i>		
PET	3	2.124081	0.708027	0.00074		
PS	3	2.099853	0.699951	0.002233		
PLA	2	1.561224	0.780612	0.002575		
ANOVA						
<i>Source of Variation</i>	<i>SS</i>	<i>df</i>	<i>MS</i>	<i>F</i>	<i>P-value</i>	<i>F crit</i>
Between Groups	0.008905	2	0.004452	2.612584	0.167205	5.786135
Within Groups	0.008521	5	0.001704			
Total	0.017425	7				

Table 36 Thymol:Menthol (1:1) Endpoint Extraction ANOVA

Anova: Single Factor						
SUMMARY						
<i>Groups</i>	<i>Count</i>	<i>Sum</i>	<i>Average</i>	<i>Variance</i>		
PET	3	2.250424	0.750141	0.007186		
PS	3	1.808397	0.602799	0.018121		
PLA	3	1.65372	0.55124	0.002807		
ANOVA						
<i>Source of Variation</i>	<i>SS</i>	<i>df</i>	<i>MS</i>	<i>F</i>	<i>P-value</i>	<i>F crit</i>
Between Groups	0.06393	2	0.031965	3.411083	0.102464	5.143253
Within Groups	0.056225	6	0.009371			
Total	0.120155	8				

1.2. Regression Reports

Table 37 PET & Decanoic Acid:Menthol (1:1) Regression Report

Equation: Hyperbola, Single Rectangular, 2 Parameter				
$f = a*x/(b+x)$				
R	Rsqr	Adj Rsqr	Standard Error of Estimate	
0.983	0.9662	0.9647	5.5693	
	Coefficient	Std. Error	t	P
a	92.214	2.0043	46.0072	<0.0001
b	0.6588	0.1367	4.8181	<0.0001

Table 38 PET & Decanoic Acid:Menthol (1:2) Regression Report

Equation: Hyperbola, Single Rectangular, 2 Parameter				
$f = a*x/(b+x)$				
R	Rsqr	Adj Rsqr	Standard Error of Estimate	
0.9918	0.9836	0.9828	3.8993	
	Coefficient	Std. Error	t	P
a	93.1897	1.3928	66.9099	<0.0001
b	0.6162	0.0922	6.6807	<0.0001

Table 39 PET & Thymol:Menthol (1:1) Regression Report

Equation: Hyperbola, Single Rectangular, 2 Parameter				
$f = a*x/(b+x)$				
R	Rsqr	Adj Rsqr	Standard Error of Estimate	
0.9851	0.9704	0.969	5.0318	
	Coefficient	Std. Error	t	P
a	90.7149	1.9237	47.1574	<0.0001
b	1.0183	0.1545	6.5899	<0.0001

Table 40 PS & Decanoic Acid:Menthol (1:1) Regression Report

Equation: Hyperbola, Single Rectangular, 2 Parameter				
f = a*x/(b+x)				
R	Rsqr	Adj Rsqr	Standard Error of Estimate	
0.9768	0.9541	0.952	5.0825	
	Coefficient	Std. Error	t	P
a	72.7804	1.9159	37.9868	<0.0001
b	0.9316	0.1856	5.0203	<0.0001

Table 41 PS & Decanoic Acid:Menthol (1:2) Regression Report

Equation: Hyperbola, Single Rectangular, 2 Parameter				
f = a*x/(b+x)				
R	Rsqr	Adj Rsqr	Standard Error of Estimate	
0.9291	0.8632	0.8583	9.3281	
	Coefficient	Std. Error	t	P
a	82.0796	7.4766	10.9782	<0.0001
b	16.7812	4.3035	3.8994	0.0005

Table 42 PS & Thymol:Menthol (1:1) Regression Report

Equation: Hyperbola, Single Rectangular, 2 Parameter				
f = a*x/(b+x)				
R	Rsqr	Adj Rsqr	Standard Error of Estimate	
0.8476	0.7184	0.7093	11.2071	
	Coefficient	Std. Error	t	P
a	62.5831	3.0606	20.4477	<0.0001
b	1.1163	0.4566	2.4446	0.0204

Table 43 PLA & Decanoic Acid:Menthol (1:1) Regression Report

Equation: Hyperbola, Single Rectangular, 2 Parameter				
f = a*x/(b+x)				
R	Rsqr	Adj Rsqr	Standard Error of Estimate	
0.9618	0.925	0.922	7.4959	
	Coefficient	Std. Error	t	P
a	89.6455	3.3019	27.1495	<0.0001
b	13.5555	3.0014	4.5164	0.0001

Table 44 PLA & Decanoic Acid:Menthol (1:2) Regression Report

Equation: Hyperbola, Single Rectangular, 2 Parameter				
f = a*x/(b+x)				
R	Rsqr	Adj Rsqr	Standard Error of Estimate	
0.9926	0.9852	0.9843	3.0714	
	Coefficient	Std. Error	t	P
a	83.947	1.6828	49.8857	<0.0001
b	14.266	1.6665	8.5603	<0.0001

Table 45 PLA & Thymol:Menthol (1:1) Regression Report

Equation: Hyperbola, Single Rectangular, 2 Parameter				
f = a*x/(b+x)				
R	Rsqr	Adj Rsqr	Standard Error of Estimate	
0.9263	0.8581	0.8524	5.6541	
	Coefficient	Std. Error	t	P
a	49.4825	2.9444	16.8058	<0.0001
b	21.9126	5.9407	3.6885	0.0011

1.3. Contact Angle Tables

Table 46 Decanoic Acid:Menthol (1:1) at 0 Seconds Contact Angle ANOVA

Anova: Single Factor						
SUMMARY						
<i>Groups</i>	<i>Count</i>	<i>Sum</i>	<i>Average</i>	<i>Variance</i>		
PET	2	19.84	9.92	0.0288		
PS	2	48.01	24.005	7.41125		
ANOVA						
<i>Source of Variation</i>	<i>SS</i>	<i>df</i>	<i>MS</i>	<i>F</i>	<i>P-value</i>	<i>F crit</i>
Between Groups	198.3872	1	198.3872	53.32954	0.01824	18.51282
Within Groups	7.44005	2	3.720025			
Total	205.8273	3				

Table 47 Decanoic Acid:Menthol (1:2) at 0 Seconds Contact Angle ANOVA

Anova: Single Factor						
SUMMARY						
<i>Groups</i>	<i>Count</i>	<i>Sum</i>	<i>Average</i>	<i>Variance</i>		
PET	2	21.69	10.845	2.22605		
PS	2	30.96	15.48	0.0008		
ANOVA						
<i>Source of Variation</i>	<i>SS</i>	<i>df</i>	<i>MS</i>	<i>F</i>	<i>P-value</i>	<i>F crit</i>
Between Groups	21.48323	1	21.48323	19.29472	0.048118	18.51282
Within Groups	2.22685	2	1.113425			
Total	23.71008	3				

Table 48 Thymol:Menthol (1:1) at 0 Seconds Contact Angle ANOVA

Anova: Single Factor						
SUMMARY						
<i>Groups</i>	<i>Count</i>	<i>Sum</i>	<i>Average</i>	<i>Variance</i>		
PET	2	28.76	14.38	0.8978		
PS	2	43.77	21.885	9.90125		
ANOVA						
<i>Source of Variation</i>	<i>SS</i>	<i>df</i>	<i>MS</i>	<i>F</i>	<i>P-value</i>	<i>F crit</i>
Between Groups	56.32503	1	56.32503	10.43148	0.083966	18.51282
Within Groups	10.79905	2	5.399525			
Total	67.12408	3				

Table 49 Decanoic Acid:Menthol (1:1) at 30 Seconds Contact Angle ANOVA

Anova: Single Factor						
SUMMARY						
<i>Groups</i>	<i>Count</i>	<i>Sum</i>	<i>Average</i>	<i>Variance</i>		
PET	2	10	5	0		
PS	2	22.64	11.32	4.5602		
ANOVA						
<i>Source of Variation</i>	<i>SS</i>	<i>df</i>	<i>MS</i>	<i>F</i>	<i>P-value</i>	<i>F crit</i>
Between Groups	39.9424	1	39.9424	17.51783	0.05262	18.51282
Within Groups	4.5602	2	2.2801			
Total	44.5026	3				

Table 50 Thymol:Menthol (1:1) at 30 Seconds Contact Angle ANOVA

Anova: Single Factor						
SUMMARY						
<i>Groups</i>	<i>Count</i>	<i>Sum</i>	<i>Average</i>	<i>Variance</i>		
PET	2	12.41	6.205	2.90405		
PS	2	14.75	7.375	0.36125		
ANOVA						
<i>Source of Variation</i>	<i>SS</i>	<i>df</i>	<i>MS</i>	<i>F</i>	<i>P-value</i>	<i>F crit</i>
Between Groups	1.3689	1	1.3689	0.838453	0.456501	18.51282
Within Groups	3.2653	2	1.63265			
Total	4.6342	3				

Table 51 PET at 0 Seconds Contact Angle ANOVA

Anova: Single Factor						
SUMMARY						
<i>Groups</i>	<i>Count</i>	<i>Sum</i>	<i>Average</i>	<i>Variance</i>		
DA:M (1:1)	2	19.84	9.92	0.0288		
DA:M (1:2)	2	21.69	10.845	2.22605		
T:M (1:1)	2	28.76	14.38	0.8978		
ANOVA						
<i>Source of Variation</i>	<i>SS</i>	<i>df</i>	<i>MS</i>	<i>F</i>	<i>P-value</i>	<i>F crit</i>
Between Groups	22.1623	2	11.08115	10.54461	0.043949	9.552094
Within Groups	3.15265	3	1.050883			
Total	25.31495	5				

Table 52 PS at 0 Seconds Contact Angle ANOVA

Anova: Single Factor						
SUMMARY						
<i>Groups</i>	<i>Count</i>	<i>Sum</i>	<i>Average</i>	<i>Variance</i>		
DA:M (1:1)	2	48.01	24.005	7.41125		
DA:M (1:2)	2	30.96	15.48	0.0008		
T:M (1:1)	2	43.77	21.885	9.90125		
ANOVA						
<i>Source of Variation</i>	<i>SS</i>	<i>df</i>	<i>MS</i>	<i>F</i>	<i>P-value</i>	<i>F crit</i>
Between Groups	78.79603	2	39.39802	6.826778	0.076458	9.552094
Within Groups	17.3133	3	5.7711			
Total	96.10933	5				

Table 53 PS at 30 Seconds Contact Angle ANOVA

Anova: Single Factor						
SUMMARY						
<i>Groups</i>	<i>Count</i>	<i>Sum</i>	<i>Average</i>	<i>Variance</i>		
DA:M (1:1)	2	22.64	11.32	4.5602		
DA:M (1:2)	2	10	5	0		
T:M (1:1)	2	14.75	7.375	0.36125		
ANOVA						
<i>Source of Variation</i>	<i>SS</i>	<i>df</i>	<i>MS</i>	<i>F</i>	<i>P-value</i>	<i>F crit</i>
Between Groups	40.76403	2	20.38202	12.4244	0.035357	9.552094
Within Groups	4.92145	3	1.640483			
Total	45.68548	5				

2. APPENDIX 2: DETAILED SIMULATION METHODOLOGY

The following methodology was written and provided by Qi Qiao and is included here as further reference to how the simulation was carried out.

2.1. Molecular Model

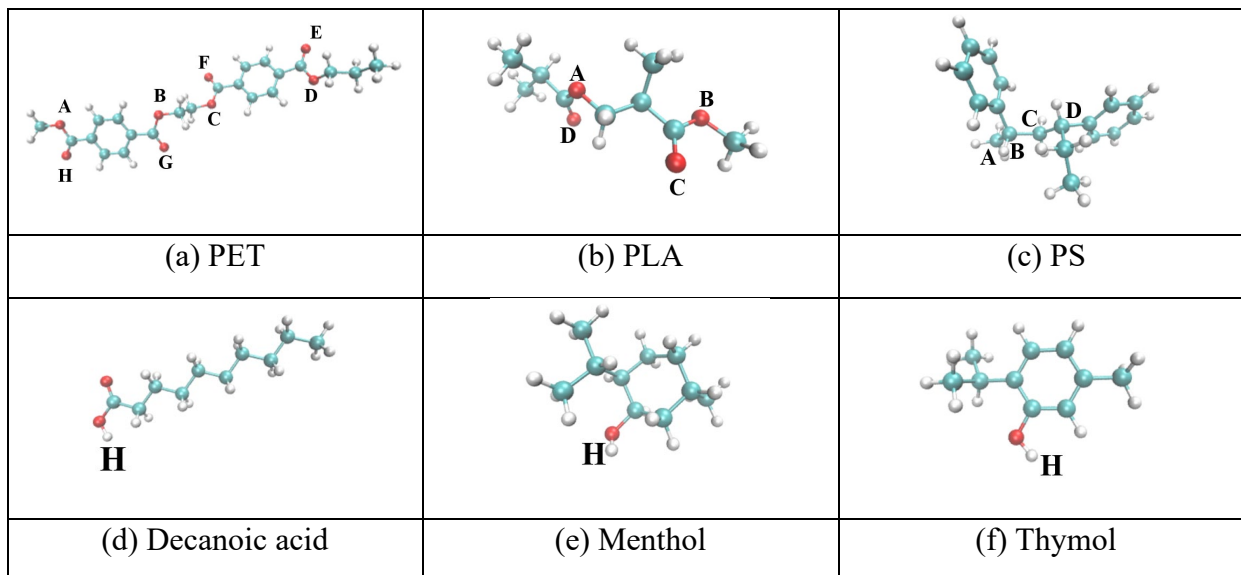


Figure 28 Molecular structures of the three plastics: (a) PET, (b) PLA, (c) PS, and three organic molecules formed the three NADESs: (d) decanoic acid, (e) menthol and (f) thymol. The molecules are shown in the CPK model (C: cyan, O: red, and H: white). All the oxygen atoms on PET and PLA, four carbon atoms on the mainchain of PS, and all hydrogen atoms on the hydroxyl groups of the three organic molecules are labelled. These labels will be used to calculate RDF.

The all-atom model was used to describe the Polyethylene terephthalate (PET), Polylactic acid (PLA), Polystyrene (PS), decanoic acid (Dec), menthol (Men), and thymol molecules, while the TIP 4P model (Jorgensen, Chandrasekhar et al. 1983) was used for the water molecules. Figure 28 shows the structures of the six molecules. The nonbonded and bonded interactions in the system were described using the OPLSAA/M force field (Robertson, Tirado-Rives et al. 2015) because this force field can properly describe the behavior of organic molecules. The force field parameters were assigned

using the Ligpargen web server (William L. Jorgensen* 2005, Dodda, Cabeza de Vaca et al. 2017, Dodda, Vilseck et al. 2017).

2.2. Simulation Detail

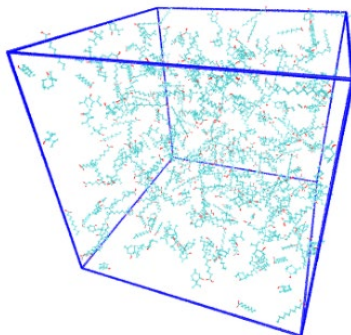


Figure 29 Snapshot of the initial configuration of PET in Dec-Men11 containing 1 PET, 200 Dec, and 200 Men molecules. Colour representations are same as in Figure 1.

The simulation systems of nine plastic-NADESs were created by placing a plastic molecule in a cubic box and filling the box with specific numbers of solvent molecules. The creation of the simulation box was fulfilled using the insert-molecule and solvate tools of GROMACS (Abraham, Murtola et al. 2015). Table 54 shows the details of the twelve NADES and water systems. Figure 29 shows the snapshot of PET in Dec-Men11.

Table 54 Components, molar ratio, and numbers of molecules in the nine plastic-NADES systems.

System label	Component A	Component B	NADES molar ratio	Total number of solvent molecules
--------------	-------------	-------------	-------------------	-----------------------------------

PET-Dec-Men11	Decanoic Acid	Menthol	1:1	400
PET-Dec-Men12	Decanoic Acid	Menthol	1:2	600
PET-Thy-Men11	Thymol	Menthol	1:1	400
PET-water	water	-	-	4115
PLA-Dec-Men11	Decanoic Acid	Menthol	1:1	400
PLA-Dec-Men12	Decanoic Acid	Menthol	1:2	600
PLA-Thy-Men11	Thymol	Menthol	1:1	400
PLA-water	water	-	-	4128
PS-Dec-Men11	Decanoic Acid	Menthol	1:1	400
PS-Dec-Men12	Decanoic Acid	Menthol	1:2	600
PS-Thy-Men11	Thymol	Menthol	1:1	400
PS-water	water	-	-	3590

This work deploys the OPLSAA/M force field (Robertson, Tirado-Rives et al. 2015) to describe bonded and nonbonded interactions in the systems. The OPLSAA/M force field has been widely used for simulating small molecules and biomolecules. The non-bonded interactions are a sum of short-range Lennard-Jones 12-6 potential and long-range coulombic potential, as shown in Equation 1. The bonded interactions are a sum of the bond, angle, and dihedral potentials, as described in the force field.

$$E_{ij}(r_{ij}) = 4\epsilon_{ij} \left(\left(\frac{\sigma_{ij}}{r_{ij}} \right)^{12} - \left(\frac{\sigma_{ij}}{r_{ij}} \right)^6 \right) + \frac{e_i e_j}{4\pi\epsilon_0 r_{ij}} \quad (1)$$

where E_{ij} is the potential energy due to the nonbonded interactions between atoms i and j , r_{ij} is the distance between atoms i and j , ϵ_{ij} is the energetic parameter, σ_{ij} is

the geometric parameter and e_i is the partial charge of atom i . The Jorgensen mixing rule is applied to obtain ϵ_{ij} and σ_{ij} for atoms belonging to different types.

A three-step simulation process is conducted for every simulation system. First, energy minimization was conducted to remove any too-close contacts between atoms. Second, three simulations, a 50-ns isobaric-isothermal (NPT, T=373 K, P= 100 KPa), a 50-ns isobaric-isothermal (NPT, T=335 K, P= 100 KPa), and a 50-ns isobaric-isothermal (NPT, T=298 K, P= 100 KPa) ensemble MD simulation (integral step = 2 fs) were conducted to let the system reach thermodynamic equilibrium. Third, a 1000-ns isobaric-isothermal (NPT, T=298 K) ensemble MD simulation (integral step = 2 fs) was conducted to collect the trajectory at a frequency of 50 ps. The Berendsen method (Berendsen, Postma et al. 1984) is used to control the temperature and pressure of the system in the second step because it allows the system to reach the desired pressure and temperature at a fast pace. The Parrinello-Rahman method (Parrinello and Rahman 1981) is used to control the pressure of the system in the third step to collect the mean square displacement (MSD). The velocity-rescaling method (Bussi, Donadio et al. 2007) is used to control the temperature of the system in the third step. The short-range van der Waals interactions use a 1.2-nm cut-off, and the long-range electrostatic interactions were calculated using the particle mesh Ewald sum. (Darden, York et al. 1993) All bonds involving H atoms were constrained during the simulations. The energy minimization and MD simulations for all the systems were conducted using Gromacs-2021 (Esquembre, Sanz et al. 2013).

3. APPENDIX 3: ADDITIONAL SIMULATION FIGURES

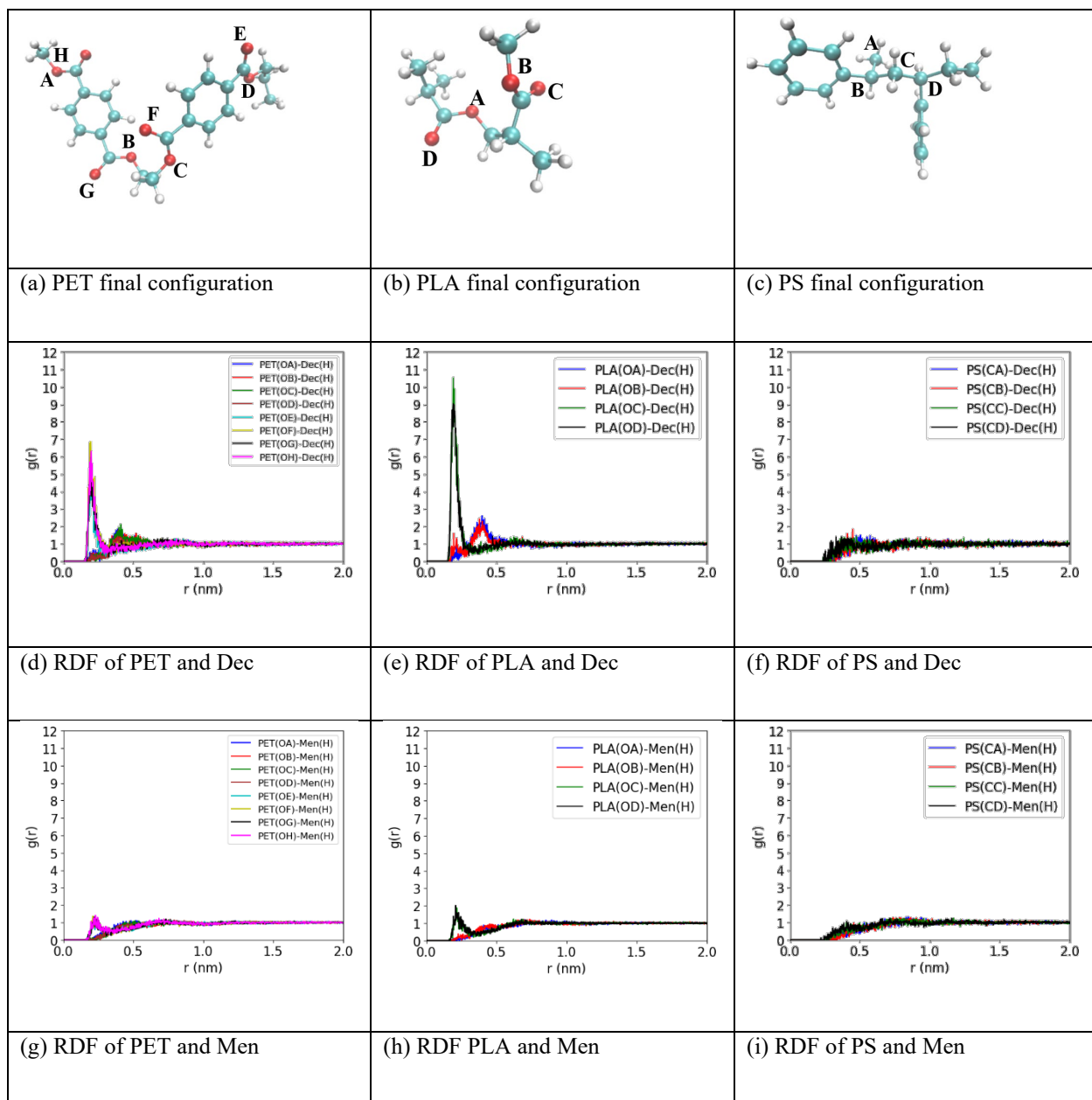


Figure 30 Final configuration and RDF results from the polymers in decanoic acid:menthol (1:2). (a)-(c) show the final configurations of PET, PLA, and PS. (d) and (e) display the oxygen-hydrogen RDF between PET and PLA respectively with decanoic acid. (f) displays the carbon-hydrogen RDF between PS and decanoic acid. (g) and (h) display the oxygen-hydrogen RDF between PET and PLA respectively with menthol. (i) displays the carbon-hydrogen RDF between PS and menthol. (This figure was provided by Qi Qiao and represents results from her simulations.)

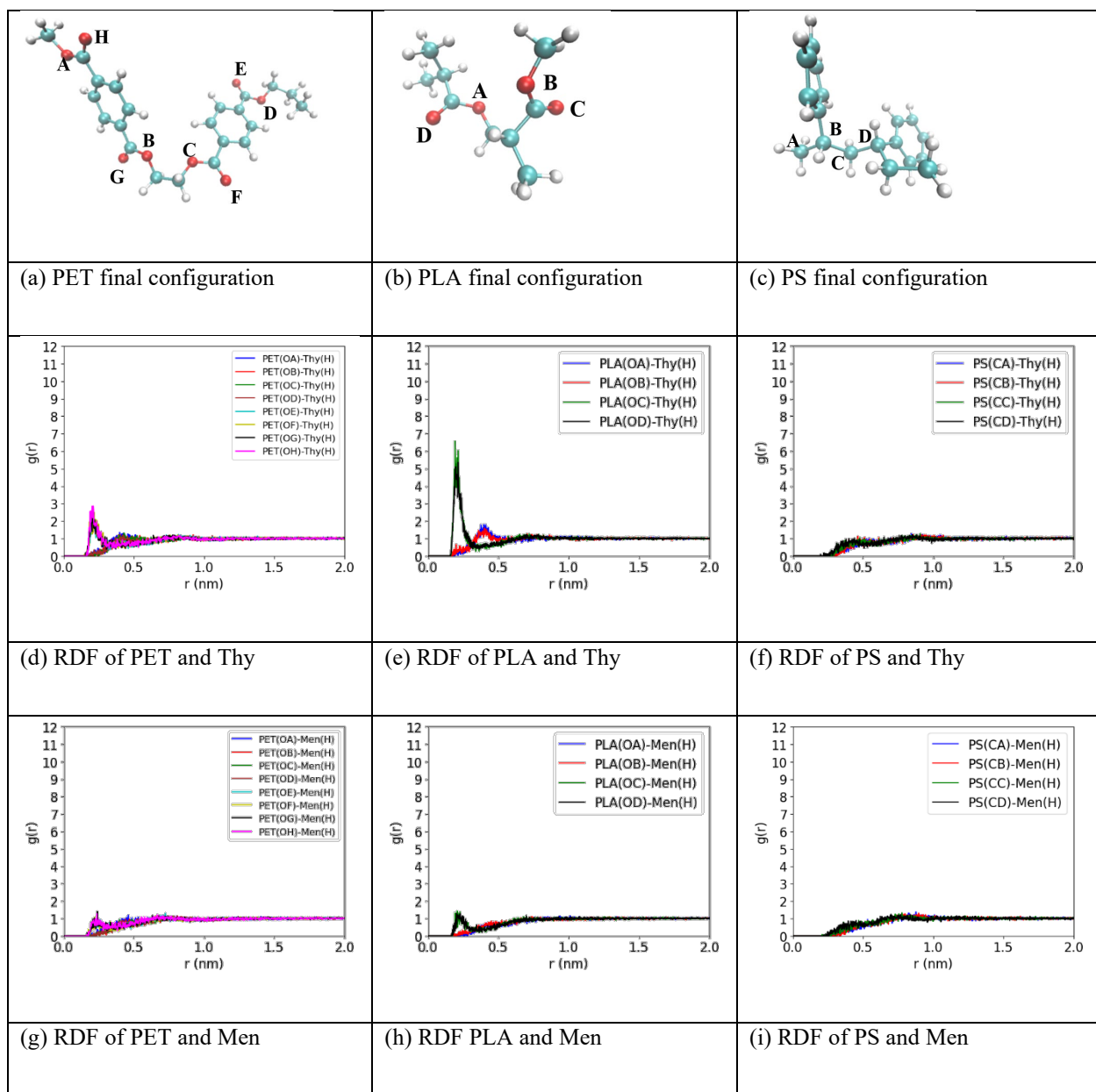


Figure 31 Final configuration and RDF results from the polymers in thymol:menthol (1:1). (a)-(c) show the final configurations of PET, PLA, and PS. (d) and (e) display the oxygen-hydrogen RDF between PET and PLA respectively with thymol. (f) displays the carbon-hydrogen RDF between PS and thymol. (g) and (h) display the oxygen-hydrogen RDF between PET and PLA respectively with menthol. (i) displays the carbon-hydrogen RDF between PS and menthol. (This figure was provided by Qi Qiao and represents results from her simulations.)

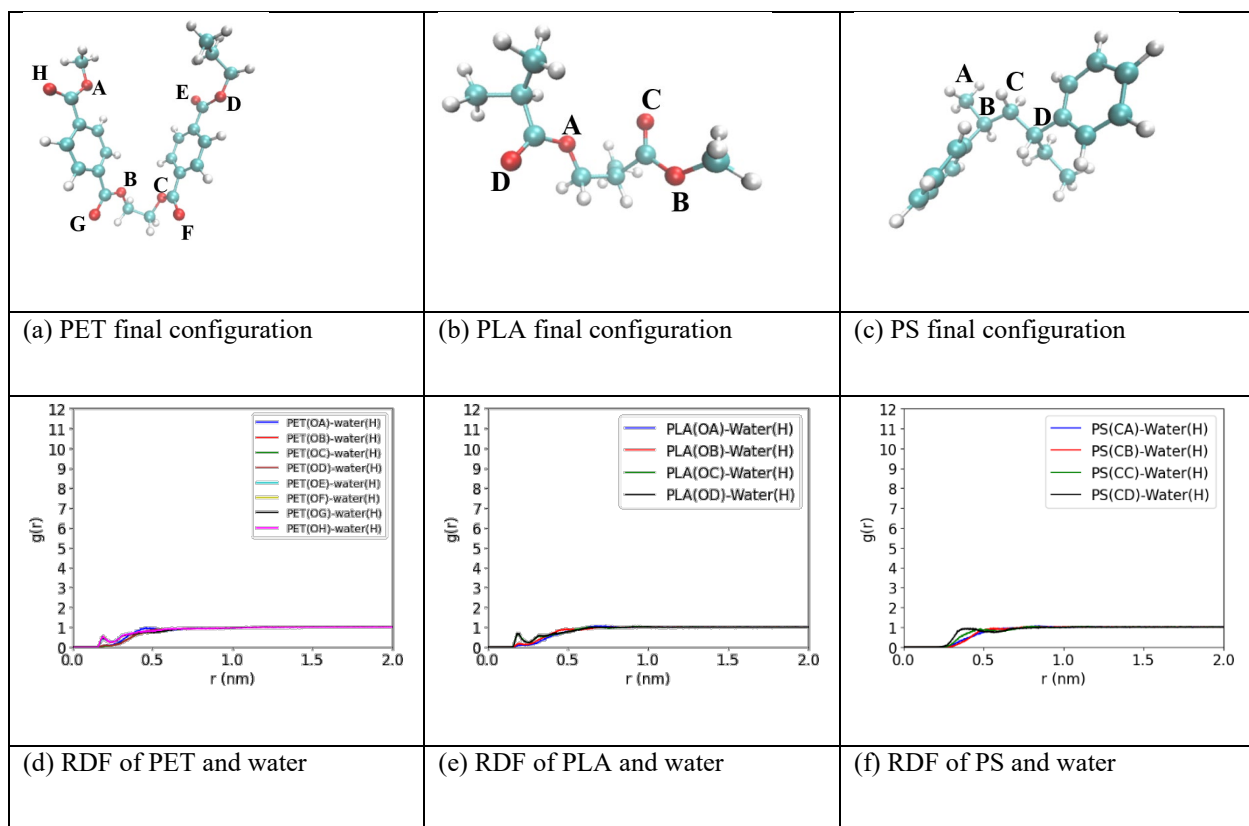


Figure 32 Final configuration and RDF results from the polymers in water. (a)-(c) show the final configurations of PET, PLA, and PS. (d) and (e) display the oxygen-hydrogen RDF between PET and PLA respectively with water. (f) displays the carbon-hydrogen RDF between PS and water. (This figure was provided by Qi Qiao and represents results from her simulations.)

REFERENCES

- Abraham, M. J., T. Murtola, R. Schulz, S. Páll, J. C. Smith, B. Hess and E. Lindahl (2015). "GROMACS: High performance molecular simulations through multi-level parallelism from laptops to supercomputers." SoftwareX **1**: 19-25.
- Abraham, M. J., T. Murtola, R. Schulz, S. Páll, J. C. Smith, B. Hess and E. Lindahl (2015). "GROMACS: High performance molecular simulations through multi-level parallelism from laptops to supercomputers." SoftwareX **1-2**: 19-25.
- Anastas, P. T. and J. C. Warner (1998). "Green chemistry." Frontiers **640**: 1998.
- Avio, C. G., S. Gorbi and F. Regoli (2017). "Plastics and microplastics in the oceans: from emerging pollutants to emerged threat." Marine environmental research **128**: 2-11.
- Berendsen, H. J., J. v. Postma, W. F. van Gunsteren, A. DiNola and J. R. Haak (1984). "Molecular dynamics with coupling to an external bath." The Journal of chemical physics **81**(8): 3684-3690.
- Bussi, G., D. Donadio and M. Parrinello (2007). "Canonical sampling through velocity rescaling." The Journal of chemical physics **126**(1): 014101.
- Cunha, S. C. and J. O. Fernandes (2018). "Extraction techniques with deep eutectic solvents." TrAC Trends in Analytical Chemistry **105**: 225-239.
- Darden, T., D. York and L. Pedersen (1993). "Particle mesh Ewald: An $N \cdot \log(N)$ method for Ewald sums in large systems." The Journal of chemical physics **98**(12): 10089-10092.
- Dodda, L. S., I. Cabeza de Vaca, J. Tirado-Rives and W. L. Jorgensen (2017). "LigParGen web server: an automatic OPLS-AA parameter generator for organic ligands." Nucleic Acids Res **45**(W1): W331-W336.
- Dodda, L. S., I. Cabeza de Vaca, J. Tirado-Rives and W. L. Jorgensen (2017). "LigParGen web server: an automatic OPLS-AA parameter generator for organic ligands." Nucleic acids research **45**(W1): W331-W336.
- Dodda, L. S., J. Z. Vilseck, J. Tirado-Rives and W. L. Jorgensen (2017). "1.14* CM1A-LBCC: localized bond-charge corrected CM1A charges for condensed-phase simulations." The journal of physical chemistry B **121**(15): 3864-3870.
- Dodda, L. S., J. Z. Vilseck, J. Tirado-Rives and W. L. Jorgensen (2017). "1.14*CM1A-LBCC: Localized Bond-Charge Corrected CM1A Charges for Condensed-Phase Simulations." J Phys Chem B **121**(15): 3864-3870.
- Erni-Cassola, G., V. Zadjelovic, M. I. Gibson and J. A. Christie-Oleza (2019). "Distribution of plastic polymer types in the marine environment; A meta-analysis." Journal of hazardous materials **369**: 691-698.
- Esquembre, R., J. M. Sanz, J. G. Wall, F. del Monte, C. R. Mateo and M. L. Ferrer (2013). "Thermal unfolding and refolding of lysozyme in deep eutectic solvents and their aqueous dilutions." Physical Chemistry Chemical Physics **15**(27): 11248-11256.
- Gangadoo, S., S. Owen, P. Rajapaksha, K. Plaisted, S. Cheeseman, H. Haddara, V. K. Truong, S. T. Ngo, V. V. Vu and D. Cozzolino (2020). "Nano-plastics and their analytical characterisation and fate in the marine environment: From source to sea." Science of the Total Environment **732**: 138792.
- Ho, B. T., T. K. Roberts and S. Lucas (2018). "An overview on biodegradation of polystyrene and modified polystyrene: the microbial approach." Critical reviews in biotechnology **38**(2): 308-320.

Ilmi, M., A. Kloekhorst, J. Winkelman, G. Euverink, C. Hidayat and H. Heeres (2017). "Process intensification of catalytic liquid-liquid solid processes: Continuous biodiesel production using an immobilized lipase in a centrifugal contactor separator." Chemical Engineering Journal **321**: 76-85.

Jem, K. J. and B. Tan (2020). "The development and challenges of poly (lactic acid) and poly (glycolic acid)." Advanced Industrial and Engineering Polymer Research **3**(2): 60-70.

Jorgensen, W. L., J. Chandrasekhar, J. D. Madura, R. W. Impey and M. L. Klein (1983). "Comparison of simple potential functions for simulating liquid water." The Journal of chemical physics **79**(2): 926-935.

Jorgensen, W. L. and J. Tirado-Rives (2005). "Potential energy functions for atomic-level simulations of water and organic and biomolecular systems." Proceedings of the National Academy of Sciences **102**(19): 6665-6670.

Kawai, F., T. Kawabata and M. Oda (2020). "Current state and perspectives related to the polyethylene terephthalate hydrolases available for biorecycling." ACS Sustainable Chemistry & Engineering **8**(24): 8894-8908.

Liu, Y., J. B. Friesen, J. B. McAlpine, D. C. Lankin, S.-N. Chen and G. F. Pauli (2018). "Natural deep eutectic solvents: properties, applications, and perspectives." Journal of natural products **81**(3): 679-690.

Makoś, P., A. Przyjazny and G. Boczkaj (2018). "Hydrophobic deep eutectic solvents as "green" extraction media for polycyclic aromatic hydrocarbons in aqueous samples." Journal of Chromatography A **1570**: 28-37.

Mattsson, K., S. Jovic, I. Doverbratt and L.-A. Hansson (2018). "Nanoplastics in the aquatic environment." Microplastic contamination in aquatic environments: 379-399.

Nguyen, B., D. Claveau-Mallet, L. M. Hernandez, E. G. Xu, J. M. Farner and N. Tufenkji (2019). "Separation and analysis of microplastics and nanoplastics in complex environmental samples." Accounts of chemical research **52**(4): 858-866.

Parrinello, M. and A. Rahman (1981). "Polymorphic transitions in single crystals: A new molecular dynamics method." Journal of Applied physics **52**(12): 7182-7190.

Peng, X., M. Chen, S. Chen, S. Dasgupta, H. Xu, K. Ta, M. Du, J. Li, Z. Guo and S. Bai (2018). "Microplastics contaminate the deepest part of the world's ocean." Geochem. Perspect. Lett **9**: 1-5.

Prathapan, R., R. Thapa, G. Garnier and R. F. Tabor (2016). "Modulating the zeta potential of cellulose nanocrystals using salts and surfactants." Colloids and Surfaces A: Physicochemical and Engineering Aspects **509**: 11-18.

Raheem, A. B., Z. Z. Noor, A. Hassan, M. K. Abd Hamid, S. A. Samsudin and A. H. Sabeen (2019). "Current developments in chemical recycling of post-consumer polyethylene terephthalate wastes for new materials production: A review." Journal of Cleaner Production **225**: 1052-1064.

Reimonn, G., T. Lu, N. Gandhi and W.-T. Chen (2019). "Review of microplastic pollution in the environment and emerging recycling solutions." Journal of Renewable Materials **7**(12): 1251-1268.

Robertson, M. J., J. Tirado-Rives and W. L. Jorgensen (2015). "Improved peptide and protein torsional energetics with the OPLS-AA force field." Journal of chemical theory and computation **11**(7): 3499-3509.

- Robertson, M. J., J. Tirado-Rives and W. L. Jorgensen (2015). "Improved Peptide and Protein Torsional Energetics with the OPLSAA Force Field." J Chem Theory Comput **11**(7): 3499-3509.
- Sinha, V., M. R. Patel and J. V. Patel (2010). "PET waste management by chemical recycling: a review." Journal of Polymers and the Environment **18**(1): 8-25.
- Van Osch, D. J., C. H. Dietz, J. van Spronsen, M. C. Kroon, F. Gallucci, M. van Sint Annaland and R. Tuinier (2019). "A search for natural hydrophobic deep eutectic solvents based on natural components." ACS Sustainable Chemistry & Engineering **7**(3): 2933-2942.
- van Osch, D. J., L. F. Zubeir, A. van den Bruinhorst, M. A. Rocha and M. C. Kroon (2015). "Hydrophobic deep eutectic solvents as water-immiscible extractants." Green Chemistry **17**(9): 4518-4521.
- William L. Jorgensen*, J. T.-R. (2005). "Potential energy functions for atomic-level simulations of water and organic and biomolecular systems." PNAS **vol. 102**(no. 19): 6665–6670.
- Wu, W.-M., J. Yang and C. S. Criddle (2017). "Microplastics pollution and reduction strategies." Frontiers of Environmental Science & Engineering **11**(1): 1-4.
- Xu, P., G.-W. Zheng, M.-H. Zong, N. Li and W.-Y. Lou (2017). "Recent progress on deep eutectic solvents in biocatalysis." Bioresources and bioprocessing **4**(1): 1-18.

VITA

Jameson Hunter

Education

Master of Science in Biosystems and Agricultural Engineering, University of Kentucky, 2021

Bachelor of Science in Biosystems and Agricultural Engineering, University of Kentucky, 2019

Professional and Research Experience

Graduate Research Assistant, *Biosystems and Agricultural Engineering*, University of Kentucky, Lexington, KY (08/2019 – present)

Undergraduate Research Assistant, *Biosystems and Agricultural Engineering*, University of Kentucky, Lexington, KY (05/2017 – 08/2019)

Professional Affiliations

American Society of Agricultural and Biological Engineers (ASABE)

American Chemical Society (ACS)

Alpha Epsilon, Honors society of ASABE

Awards and Honors

Alpha Epsilon treasurer (2019 – 2020)

Graduated *Summa cum laude* for Bachelor of Science from the University of Kentucky in Biosystems and Agricultural Engineering

Dean's List (Fall 2015 to Spring 2019)